The behaviour of Cu and Zn isotopes during soil development: Controls on the dissolved load of rivers

Author(s):
Vance, Derek; Matthews, Alan; Keech, Andrew; Archer, Corey; Hudson, Gordon; Pett-Ridge, Julie; Chadwick, Oliver A.

Publication date:
2016-12-16

Permanent link:
https://doi.org/10.3929/ethz-b-000122649

Originally published in:
Chemical Geology 445, https://doi.org/10.1016/j.chemgeo.2016.06.002

The behaviour of Cu and Zn isotopes during soil development: controls on the dissolved load of rivers

Derek Vance[1*], Alan Matthews[2], Andrew Keech[3], Corey Archer[1], Gordon Hudson[4], Julie Pett-Ridge[5] and Oliver A. Chadwick[6]

[1] Institute of Geochemistry and Petrology, Department of Earth Sciences, ETH Zürich, NW D81.4, Clausiusstrasse 25, 8092 Zürich, Switzerland.

[2] Institute of Earth Sciences, Hebrew University of Jerusalem, 91904 Jerusalem, Israel.

[3] Department of Earth Sciences, University of Bristol, Wills Memorial Building, Queens Road, Bristol BS8 1RJ, UK.

[4] James Hutton Institute, Craigiebuckler, Aberdeen, AB15 8QH, UK.

[5] Department of Crop and Soil Science, Oregon State University, 3041 Ag & Life Sciences Building, Corvallis, OR 97331, USA.

[6] Department of Geography, University of California, Santa Barbara, CA 93106-4060, USA.

* Corresponding author: derek.vance@erdw.ethz.ch.

Highlights

- Light Cu, and unfractionated Zn, isotopes retained in oxic soils.
- Development of anaerobic conditions can lead to loss of this signature.
- Mineral aerosol addition and biological cycling overprint weathering processes.
- Oxic soils contain Cu-Zn isotopes complementary to riverine dissolved pool.
- Mass balance suggests ultimate fate of complementary soil signature in sediments.

Abstract

The stable isotopes of copper (Cu) and zinc (Zn) are finding increasing applications in surface Earth geochemistry. An important early observation is that aqueous pools of Cu (rivers and oceans) are isotopically heavier than rocks of the continental crust. For Zn, the global average δ^{66}Zn for rivers is identical to estimates of the upper continental crust, but the oceans are slightly heavier. Here, we study Cu and Zn abundances and isotopes in soils to assess how processes in the weathering environment control isotopic values of rivers, and ultimately the oceans. We investigated a range of soils developed on granitoid (Scotland) and basaltic (Hawaiian Islands) rock substrates, representing soil development times from 0.1 to 400 kyr, mean annual temperatures of 6-16°C, and mean annual precipitation (MAP) of 1060-5050mm.

Soils developed on the island of Maui over 400 kyr and under high rainfall show the clearest chemical weathering signatures. Here, in oxic soils, Cu and Zn are both depleted by 50-90%, with preferential loss of heavy Cu (δ^{65}Cu up to 1.2‰ lower than parent material), and small shifts in δ^{66}Zn. We attribute this to equilibrium fractionation between aqueous organic species that are removed from the soil versus sorption to residual Fe-oxyhydroxides. In soils that are 0.1-150 kyr old in Scotland and Hawaii, this same pattern is overprinted by biological cycling and the addition of mineral aerosol Cu and Zn with heavier isotope compositions. In reducing soils on Maui, developed under the highest rainfall, Cu and Zn are almost completely stripped from the soil, leaving a very small residual pool with δ^{65}Cu and δ^{66}Zn values that range from those for the oxic soils back to and beyond parent material. This removal of the light sorbed Cu seen in oxic soils is attributed to the dissolution of Fe oxides under anaerobic conditions, perhaps microbially mediated, leaving a very small residual isotopically heavier pool.

Overall these data suggest that processes in soils create significant variability in Cu isotopes, with the heavy isotope exported from oxic soils. In contrast, small isotope fractionations of Zn are generated in the soil environment. These observations are consistent with those made previously for Cu and Zn isotopes in rivers. But the maximum amount of Cu and Zn stored by world soils equates to only 30-130 years of the dissolved riverine flux. Soils cannot be the ultimate repository of the residual Cu and Zn required to balance the riverine flux, and this must ultimately reside in the erosive products of soil formation in continental and ocean margin sediments.

Keywords: chemical weathering, geochemistry, metal stable isotopes, soils, rivers.

1. Introduction

The dissolved pool of the transition metals in rivers and the oceans is almost always isotopically heavy relative to the rocks of the continents. This observation was first made for molybdenum (Mo) isotopes in the oceans (e.g. Barling et al., 2001; Nakagawa et al., 2012), and was followed up by the same finding for Mo in world rivers (Archer and Vance, 2008; Neubert et al., 2011; Voegelin et al., 2012). Since then the same observation has been made for Cu and Ni isotopes in rivers and seawater (Vance et al., 2008; Cameron and Vance, 2014; Takano et al., 2014; Thompson and Ellwood, 2014). In contrast, a recent survey of Zn isotopes in large and small rivers (Little et al., 2014a) finds a global discharge-weighted flux to the oceans that is indistinguishable from estimates of the isotope composition of the upper continental crust. Archer and Vance (2008) discussed two possible causes of the heavy metal isotope composition of rivers: isotope fractionation in soils due to the retention of light isotopes on Fe-Mn oxyhydroxide surfaces in soils, analogous to the process driving the oceans towards heavy Mo isotope compositions (Barling an Anbar, 2004; Wasylenki et al., 2011), or the sorption of light isotopes to oxyhydroxides during transport in rivers themselves. Though these authors favoured the former explanation, a significant problem lies in the size of the light reservoir in global soils that is required to balance the dissolved riverine flux of heavy metal isotopes. Vance et al. (2008), in addition to documenting heavy Cu isotope compositions dissolved in rivers, also showed that light isotope compositions in the particulate phase in one small river roughly balanced the dissolved pool, and suggested that this Cu isotope separation resulted either from partitioning of the heavy isotope into strong organic complexes in the dissolved pool or a postulated preference of Fe-Mn oxyhydroxides for the light isotope, or both acting together.

Whether isotope separation of the transition metals predominantly occurs in rivers or not, it almost certainly begins in soils. Our focus here is Cu and Zn isotopes, with their contrasting behaviour in rivers noted above. Studies of Zn isotopes in soils have partly focused on their potential utility as tracers of anthropogenic contamination (e.g. Weiss et al., 2007; John et al., 2007; Chen et al., 2008; Sivry et al., 2008; Thapalia et al., 2010; Juillot et al., 2011), and this may be a confounding factor in any attempt to understand natural processes such as chemical weathering. Viers et al. (2007) conducted a study of Zn isotopes in a "pristine" tropical watershed in Cameroon and found significant isotope variation that was attributed to natural abiotic and biological processes. Cu is probably less prone to anthropogenic effects in environmental samples (e.g. Chen et al., 2014). Bigalke et al. (2010a) studied Cu isotopes in soils variably affected by stagnant water, including features such as variations in non-crystalline Fe oxides within the profile. They observed a

transition from light isotope enrichment to heavy isotope enrichment as water-logging led to anaerobic conditions. Bigalke et al. (2011) studied oxic Cambisols and Podzols, again documenting significant Cu isotope fractionation, with δ^{65}Cu between -0.57 and +0.44‰.

Here we present data for soil profiles from Hawaii and Scotland, covering both granitoid and basaltic substrates, incorporating a range of soil development times from 0.1-400 kyr, and a range of mean annual rainfall amounts, from ~1100-5000mm. Our large-scale objective is to assess the extent to which Cu and Zn isotope behaviour in soils are consistent with the riverine data outlined above. In doing so, however, we document the variety of processes in these soils that control Cu and Zn and their isotopes: not just the impact of removal by weathering but also the effects of redox transitions on sorption substrates, organic ligands, and atmospheric addition of these metals. Our results confirm the role of both aqueous organic complexes and Fe-Mn oxyhydroxides in controlling the isotopic composition of Cu and Zn retained in soil and released to rivers.

2. Settings and samples

Samples for this study derive from two well-studied field locations, representing contrasting lithologies, soil development times, and climate (Figures 1 and 2).

2.1 Glen Feshie chronosequence, Scotland

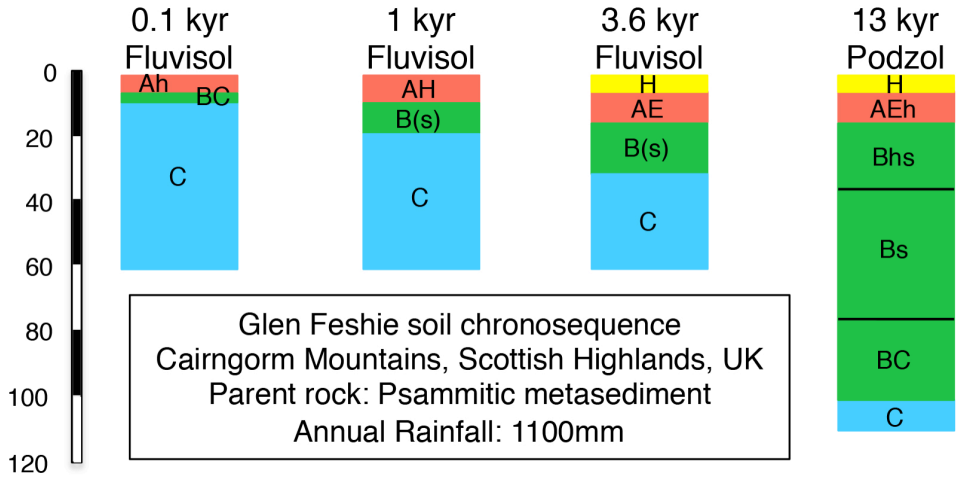

Figure 1: Schematic of the Glen Feshie soil profiles studied here, with their ages and soil types at the top. Soil types, horizons and ages from Bain et al. (1993) and Hodson et al. (1998). Depth scale at left is in cm.

The ***Glen Feshie chronosequence*** (Fig. 1) is developed on a generally "granitoid" substrate in Glen Feshie, Scotland, UK. Glen Feshie is a north-south trending valley (57°02'N, 3°53'W) forming the

western boundary of the Cairngorm Mountains in the Scottish highlands. The climate is "sub-arctic" (Helliwell et al., 1998), with mean monthly temperatures ranging from 1.2°C in February to 10.3°C in July, and mean annual precipitation of ~1100mm. The soil chronosequence is developed on four alluvial terraces deposited since the deglaciation of Scotland at ~13 ka. It was identified by Robertson-Rintoul (1986b) who identified 5 different clusters of soils, each corresponding to a terrace formation event. The chronosequence is well characterised for chemistry, mineralogy, weathering rate and texture (Bain et al., 1993; Hodson et al., 1998; Hodson and Langan, 1999; Lee et al., 2008). Maximum durations of soil development on the alluvial terraces have been estimated by ^{14}C dating and soil stratigraphy, and give a range in age for the four studied profiles of 0.1 – 13 ka (in radiocarbon years, Bain et al., 1993). The three youngest soils are classified as fluvisols and the oldest as a humo-ferri podzol, according to the FAO classification (Hodson et al., 1998).

The parent material of the chronosequence is predominantly psammitic schist with a small granitic component (10-15%; Roberston-Rintoul, 1986a). Each of the terraces in the chronosequence are considered to share similar parent materials based upon C-horizon chemistry (Bain et al., 1993). As the terraces are alluvial in origin the parent material is likely to have undergone weathering during erosion of the original rock and transport of the gravels prior to deposition. The extent of this weathering is unknown, but it is expected to have affected the parent material of each chronosequence member to the same extent. Textural evidence suggests minimal weathering of primary biotite occurred during transport of alluvium in Glen Feshie as biotite grains are still clearly visible in river alluvium samples, mica is abundant in the clay fraction, and no vermiculite (the weathering product of biotite), is observed in the youngest soil (0.1 ka; Bain et al., 1993). Vegetation is dominated by dry *Calluna* moor of *Calluna vulgaris, Vaccinium myrtillus* and hypnaceous mosses with additional lichen rich *Calluna* moor, *Agrostis-Festuca* acid grassland and *Betula* woodland (Robertson-Rintoul, 1986a).

2.2 Chronosequence and climosequences, Hawaiian Islands

We have analysed a variety of soil profiles from the Hawaiian Islands, all having a basaltic substrate but varying in soil development times and climate (Fig. 2).

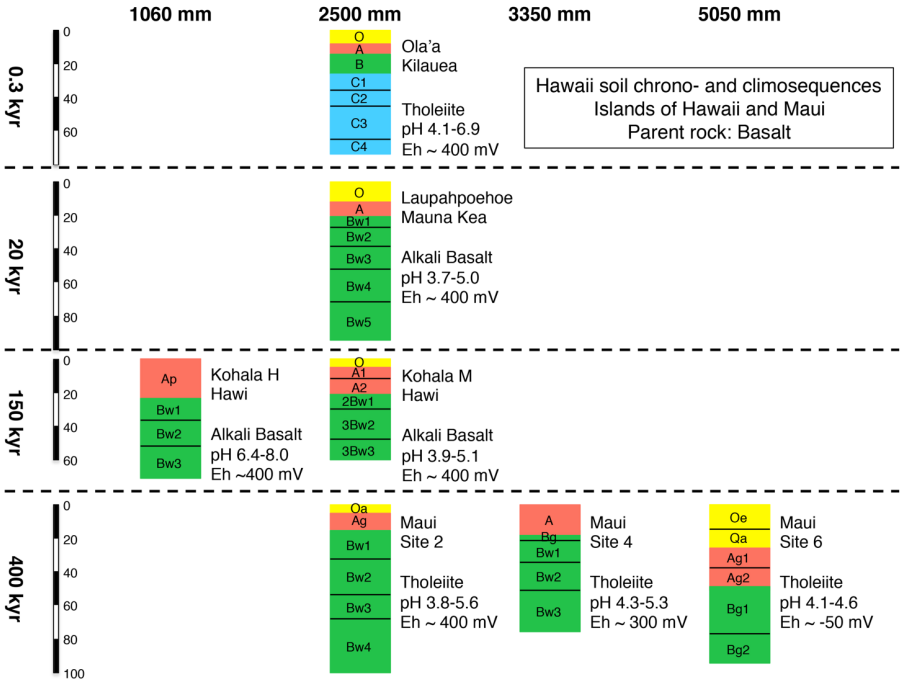

Figure 2: Schematic of Hawaiian soil profiles studied, representing a range of different ages and mean annual rainfalls, but all developed on a basaltic substrate (see text for sources of data). The age gradient from 0.3-150 kyr at 2500mm is part of the LSAG chronosequence (Crews et al., 1995). Note that the top 25 cm of the 1 m profile sampled at Laupahoehoe consists of a younger less weathered 5 ka ash lying on top of ca 20 ka tephra (Kennedy et al., 1998; Chadwick et al., 2009). Depth scale at left is in cm. The 0-150 kyr soils are Andisols (Pett-Ridge et al., 2007) while the 400 kyr Maui soils are classified as (Schuur et al., 2001): Inceptisol (Maui 2 and 6) and Andisol (Maui 4).

The ***Long Substrate Age Gradient (LSAG) chronosequence*** was established by Crews et al. (1995) and well characterized by subsequent studies (Chadwick et al., 1999; Chorover et al., 1999; Hotchkiss et al., 2000; Kennedy et al., 1998; Kurtz et al., 2000; Kurtz et al., 2001; Vitousek, 2004; Monastra et al., 2004; Torn et al., 1997; Pett-Ridge et al., 2007). The chronosequence consists of six sites located on the islands of Hawaii, with substrate soil ages ranging from 0.3 ka to 4.1 Ma. In the present study, Cu and Zn isotope compositions and soil chemistry were examined at three of these soil sites on the island of Hawaii (Fig. 2). The three studied profiles, Ola'a (0.3 ka), Laupahoehoe (~5-20 ka) and Kohala M (~150 ka) formed at similar conditions of ~ 1200m elevation, minimal slope gradient (6%), 2500 mm present–day rainfall and 16°C surface temperatures. The Ola'a soil volcanic substrate is tholeiite, while the Laupahoehoe soil substrate is late-stage alkaline basalts (hawaiite and mugearite). The Kohala M site (150 ka) (Fig. 2) is in a pasture and is similar to, but not the exact Kohala site sampled along the LSAG. The specific samples studied here are from the same profiles documented in Pett-Ridge et al. (2007).

187 The tephra substrates of these soils have ages of 0.3 ka (Ola'a rainforest, Kilauea), 5-20 ka
188 (Laupahoehoe Volcanics, Mauna Kea), and 150 ka (Hawi Volcanics, Kohala M). The uncertainties
189 surrounding the exact ages of the parent material for these sites are discussed in Vitousek (2004).
190 An age of 2.1 ka was originally assigned to the Ola'a site, but a later re examination determined that
191 the soil is developed on a 0.3 ka ash-fall (Keanakakoi Ash) on top of a 2.1 ka substrate (McPhie et
192 al., 1990). Laupahoehoe soils are formed on a tephra deposit that is at least 2-3 m thick and is a
193 cumulic deposit consisting of several buried soils. The top 25 cm of the 1 m profile sampled in this
194 study consists of a younger less weathered 5 ka ash lying on top of ca 20 ka tephra (Kennedy et al.,
195 1998; Chadwick et al., 2009). The Kohala M site is also part of the rainfall gradient studied by
196 Teutsch et al. (1999) and Chadwick et al. (2003). The profile studied here is described in Chadwick
197 et al (2003).
198
199 Ola'a, Laupahoehoe and Kohala M all receive approximately 2500 mm yr^{-1} of orographic rainfall,
200 dominantly associated with northeasterly trade winds. Soil sites older than 20 ka have been subject
201 to cooler and drier conditions than present due to changes in the elevation of the inversion layer and
202 island subsidence (Hotschkiss et al., 2000). Based on data published for the climosequence on Maui
203 by Schuur et al. (2001) (see Chadwick and Chorover, 2001; Pett-Ridge et al., 2007), Eh conditions
204 in the present-day soils are estimated at ~ 400 ± 100 mV. Soil mottling suggests that, though the
205 soils are well aerated most of the time, they are subjected to occasional declines in Eh values during
206 and after high rainfall events. The Ola'a and Laupahoehoe sites were sampled in intact rainforest
207 composed of a dominant canopy tree, O'hia (*Metrosideros polymorpha*), whereas the Kohala soil
208 was sampled in a pasture site whose forest had been cleared about 100 years ago.
209
210 Though the Hawaiian Islands are remote from potential dust sources, previous mineralogical,
211 chemical and isotopic studies have documented significant additions of trace elements in Hawaiian
212 soils due to long-range atmospheric transport and deposition of Asian dust (e.g. Kennedy et al.,
213 1998; Teutsch et al., 1999; Kurtz et al., 2001; Stewart et al., 2001; Huh et al., 2004; Monastra et al.,
214 2004; Scribner et al., 2006; Pett–Ridge et al., 2007; Chadwick et al., 2009; Mikutta et al., 2009).
215 These studies show that atmosphere-transported metal input may account for a large, or even
216 dominant, portion of the overall metal budget in 150 kyr soils. For example, the Laupahoehoe and
217 Kohala M soils have up to 15% and 40% quartz, respectively, with smaller amounts of mica and K-
218 feldspar, accumulated from eolian sources (Kurtz et al., 2001).
219
220 In addition to the profiles described in detail above, we have also studied a low rainfall site

(1060mm), also 150 kyr in age, at Kohala (Kohala H) (Chadwick et al., 2003). This soil profile is developed on the same alkali basalt substrate as Kohala M, and over the same length of time (150 kyr), thus creating a two-point climosequence at this age for comparison with a wetter climosequence on Maui.

The ***Maui climosequence*** consists of soil profiles developed on the 410 kyr shield-building Kula Volcanic Series on the northwest slope of Haleakala, is described in detail by Miller et al. (2001), Schuur et al (2001a,b), Scribner et al. (2006), and has previously been the subject of iron and molybdenum isotope studies (Thompson et al., 2007; Siebert et al., 2015). Soil elevation is ~1300mm and <5% slopes lead to low erosion rates and timescales of pedogenesis similar to the age of the underlying basalt. Mean annual temperatures are ~16°C. Three of the 8 sites across the full rainfall gradient are studied here: Site 2 (mean annual precipitation = 2450mm), Site 4 (3350mm) and Site 6 (5050mm). These precipitation levels, as well as differences between sites, have probably persisted throughout the Holocene (Hotchkiss et al., 2000; Chadwick et al., 2003). The sites have undisturbed native forest dominated by the same single tree species as for the LSAG chronosequence, *Metrosideros polymorpha*.

A particular feature of the Maui sequence (see Fig. 2) is a well-characterized redox gradient and its impact on the fate of oxidized Fe minerals (Schuur et al., 2001; Thompson et al., 2011). At the lowest rainfall Site 2, the relatively well-drained soils contain abundant Fe(III) minerals. At rainfall levels around 3000mm a redox threshold is crossed leading to waterlogged soils, so that sites 4 and 6 are characterized by periods of suboxic conditions leading to mobilization of the oxidized Fe via reductive dissolution of Fe oxyhydroxides (Chadwick and Chorover, 2001; Miller et al., 2001). Soil organic matter content increases across this redox gradient, as degradation is suppressed in anaerobic conditions, from about 15% carbon at Site 2 to about 25% at Site 6 (Schuur et al., 2001). Addition of material via mineral aerosol dust is also a potential complication for these old soils. Profiles of quartz (absent from basaltic parent rock) concentrations show a sharp maximum in quartz concentrations (22 wt%) at 10 cm at Site 2, but very low concentrations elsewhere in this profile. At the wetter sites this peak is less pronounced (about 18% at Site 4 and about 13% at Site 6) but significant concentrations of quartz persist further down the profile (50cm at Site 4 and 80 cm at Site 6).

3. Methods

255 Glen Feshie soils were sampled (~1 kg) from each soil horizon at the same locations as in Bain et
256 al. (1993). Soil samples were dried at 60°C for 48 hours and sieved at 2mm. A representative
257 sample of the fine fraction (10-15g) was taken and powdered in an agate mill. River alluvium
258 samples were collected from the river bed using a clean trowel, and rock samples from outcrop on
259 the valley floor. The alluvium was collected at Glen Feshie because it will be closer to the parent
260 material of the soils, which are developed on alluvial terraces. Rock and alluvium samples were
261 crushed to sub-mm size in a jaw crusher. A representative (10-15g) aliquot of all samples was then
262 taken and powdered in an agate mill. Plant samples (Heather (*Calluna vulgaris*) and common grass)
263 were also collected from the 1 and 13 kyr sites. Plant samples were separated into root, stem and
264 leaf fractions for Cu and Zn isotope analysis, cleaned with 18.2Mohm MQ water and dried at 60°C
265 for three days. Finally, samples of the River Feshie were collected for dissolved load analysis, in
266 low-density poly-ethylene bottles. Water samples were immediately filtered at 0.2 μm and acidified
267 to pH 2 prior to storage. Hawaiian soil samples, 6-8 samples per profile, come from pits down to
268 bedrock or 1m, were sieved at 0.2mm, and dried at 105°C for 48 hours (Pett-Ridge et al., 2007;
269 Scribner et al. 2006).

270 Soil, river alluvium and rock samples were digested on a hotplate with a 4:1 mixture of
271 concentrated HF and HNO_3. Plant samples were also dry-ashed at 500°C, before digestion using
272 HNO_3, H_2O_2 and HCl. River Feshie water samples were evaporated to dryness and the residue re-
273 dissolved in concentrated nitric acid to oxidise organic matter. Procedures for the major and trace
274 element analysis of rocks, soils and waters in our laboratory, as well as those for the isotopic
275 analysis of Cu and Zn, have been thoroughly documented in previous publications (e.g. Archer and
276 Vance, 2004; Vance et al., 2008; Little et al., 2014a). Only a brief summary is given here. An
277 aliquot of each sample was taken for major and trace element concentration analysis, on a Thermo-
278 Fisher Element XR sector-field inductively-coupled-plasma mass spectrometer at ETH Zürich.
279 Measured intensities were converted to concentrations using a single-point calibration relative to an
280 in-house primary standard, using indium-doping for internal standardisation. Accuracy and
281 precision were assessed using two secondary multi-element standards: National Research Council
282 of Canada river standard SLRS5, and USGS shale standard SGR1. The concentrations obtained
283 matched certified values to within 5-10% for most of the elements of interest here. For Pb we obtain
284 a value for SLRS5 (but not SGR1) that is 20% lower than the certified value (c.f. some but not all
285 laboratories in the Yeghicheyan et al., 2013 compilation). Two sigma uncertainties for repeat
286 analyses of these standards during the period when the samples studied here were run (n = 14 for
287 both standards) were less than 7%, except for Nb (11-15%).

Following concentration analysis an aliquot of the remaining solution was doped with a ^{64}Zn-^{67}Zn double spike (Bermin et al. 2006; Zhao et al., 2014), and Cu and Zn purified using a two-stage anion-exchange via the Bio-Rad AG MP-1M resin, using procedures described in detail previously (Archer and Vance, 2004; Vance et al., 2008; Little et al., 2014a), and including data for standard reference materials. Isotopic analyses were performed using a ThermoFinnigan Neptune multi-collector inductively-coupled-plasma mass spectrometer (MC-ICP-MS) at the University of Bristol. Cu was introduced to the mass spectrometer using a glass spray-chamber (Stable Introduction System, Elemental Scientific Inc, Omaha, NE, USA) and instrumental mass discrimination was corrected using standard-sample bracketing (Archer and Vance, 2004; Vance et al., 2008; Little et al., 2014a). Zinc isotopes were introduced using an Aridus, and mass discrimination corrected using the double spike (Bermin et al. 2006; Zhao et al. 2014). All Cu and Zn isotopic compositions are given in standard notation as follows relative to the NIST SRM976 and JMC Lyon Zn standards respectively:

$$\delta^{65}Cu = 1000\left[\frac{(^{65}Cu/^{63}Cu)_{sample}}{(^{65}Cu/^{63}Cu)_{SRM976}} - 1\right]$$

$$\delta^{66}Zn = 1000\left[\frac{(^{66}Zn/^{64}Zn)_{sample}}{(^{66}Zn/^{64}Zn)_{Lyon\ JMC}} - 1\right]$$

Long-term reproducibility of isotopic analyses were ≤ 0.09‰ and ≤ 0.07‰ for Cu and Zn respectively. This was assessed for Cu based on repeat measurements of a secondary standard (standard AM, measured at Bristol, Jerusalem and Zurich and with $\delta^{65}Cu$ = +0.11). Zn reproducibility was assessed through repeat analyses of spiked JMC Lyon standards (mean $\delta^{66}Zn$ = 0.01‰ ± 0.07 (±2σ; n=57)). In addition, during the course of this study we performed duplicate analyses of 11 various soil samples for Cu and Zn isotopes (completely separate digestion and analysis), though 9 of these were sequential extractions with the attendant variability associated with the leaching process. Despite this the average reproducibility was ±0.11 for both $\delta^{65}Cu$ and $\delta^{66}Zn$. Internal errors obtained from the mass spectrometric analysis were always substantially lower than long-term reproducibility, and it is the latter that is given as the uncertainty in the footnotes to the tables in this paper. Procedural blanks for sample digestion and Cu and Zn separation were <1ng and 2ng respectively, with mean isotopic compositions of 0.0‰ and +0.3‰ respectively. These blanks would lead to insignificant corrections to sample isotopic compositions and none were applied.

In order to quantify net loss or gain of an element relative to the parent material, in a procedure that eliminates the impact of density changes during soil development, we use the tau parameter (τ) of Chadwick et al. (1990). This is defined as the fraction of an element of interest (*i*) lost from, or added to, a soil horizon relative to an immobile index element (*j*):

$$\tau_{i/j} = \left[\frac{(C_i/C_j)_h}{(C_i/C_j)_p} - 1 \right]$$

where C is concentration, subscript *h* refers to the soil horizon under consideration and subscript *p* to the concentration in the unweathered parent material. Tau values greater than zero denote addition of the element of interest relative to the immobile element and values less than zero loss. Integrated tau values for the entire soil profile can identify net additions – or loss – from the soil profile as a whole. In our calculation of integrated tau we include the O horizon because plant growth should not add Cu or Zn to the soil, merely relocate them. A detailed study of Hawaiian soils (Kurtz et al., 2000) identified niobium (Nb) as the least mobile element, so we use it here for both Hawaii and Scotland. This approach assumes that a good estimate of the chemistry of the parent material is available. In the case of the Glen Feshie soils studied here, the fact that they probably underwent an earlier cycle of erosion and weathering before the material was deposited on the current river terraces suggests that local rocks may not be an appropriate reference. Thus, we choose here to reference to samples of river alluvium collected from the river draining the valley where the soils occur. For the Hawaiian samples, parent rock major elements and Nb values come from previous soil studies. - Ziegler et al. (2005) for LSAG, Scribner et al. (2006) for Maui. Cu, Zn, Mn and Pb concentrations derive from analyses of tholeiitic and alkali basalts in the literature, as detailed later in the appropriate tables.

Table 1: Mass balance (t) calculations, Cu and Zn concentration and isotope data, for the Glen Feshie chronosequence, Scotland.

Sample	Horizon	Depth (cm)	τ_{Na}[1]	τ_{Al}	τ_{Fe}	τ_{Mn}	τ_{P}	τ_{Pb}	[Cu] ppm	τ_{Cu}	$\delta^{65}Cu$[3]	[Zn] ppm	τ_{Zn}	$\delta^{66}Zn$
0. 1 kyr														
641	Ah	2.5	-0.23	-0.17	0.01	0.32	0.23	0.00	3.6	0.15	-0.26	24	0.03	0.25
642	BC	6.5	-0.32	-0.28	-0.10	0.14	0.34	-0.19	2.4	-0.15	-0.37	17	-0.19	0.26
643	C	25	-0.19	-0.13	0.06	0.17	0.30	-0.14	3.4	-0.10	-0.34	27	-0.05	0.27
Integrated			**-0.20**	**-0.14**	**0.05**	**0.19**	**0.30**	**-0.12**		**-0.07**	**-0.33**		**-0.04**	**0.27**
1 kyr														
659	AH	5	-0.57	-0.53	-0.30	-0.36	0.07	-0.16	5.3	-0.06	0.03	24	-0.41	0.30
660	B(s)	15.5	-0.12	-0.17	0.02	-0.11	0.27	-0.10	4.8	0.35	-0.33	23	-0.12	0.30
661	C	45	0.01	-0.04	0.10	-0.03	0.29	-0.10	4.4	0.26	-0.26	25	-0.05	0.35
Integrated			**-0.07**	**-0.12**	**0.04**	**-0.08**	**0.26**	**-0.11**		**0.24**	**-0.23**		**-0.10**	**0.34**
3.6 kyr														
644	H	3.5	-0.27	-0.17	-0.51	-0.50	5.34	5.50	5.0	5.91	-0.24	11	1.06	0.13
645	AE	13	-0.31	-0.24	0.25	0.49	0.77	-0.13	4.1	0.26	-0.37	17	-0.28	0.12
646	B(s)	30	-0.13	-0.10	0.15	-0.30	0.33	-0.14	3.9	0.09	-0.33	30	0.12	0.30
647	C	57	-0.10	-0.13	0.08	-0.13	0.24	-0.15	4.0	0.13	-0.36	27	0.04	0.32
Integrated			**-0.14**	**-0.14**	**0.08**	**-0.11**	**0.62**	**-0.14**		**0.14**	**-0.35**		**0.01**	**0.29**
13 kyr														
653	H	3	-0.47	-0.36	0.00	-0.54	1.81	3.01	2.8	0.74	-0.15	14	0.16	0.07
654	AEh	13	-0.47	-0.23	0.23	-0.57	0.80	0.22	3.0	0.17	-0.06	18	-0.06	0.21
655	Bhs	25	-0.42	-0.23	-0.02	-0.61	0.05	-0.16	2.6	-0.16	-0.37	18	-0.22	0.17
656	Bs	45	-0.31	-0.03	0.50	-0.49	-0.12	-0.24	4.1	0.16	-0.26	27	0.01	0.22
657	BC	75	0.04	0.05	0.24	-0.28	-0.54	-0.05	4.9	0.69	-0.22	20	-0.07	0.33
658	C	102	-0.03	-0.05	0.12	-0.32	-0.54	-0.05	5.4	0.68	-0.26	21	-0.13	0.25
Integrated			**-0.19**	**-0.07**	**0.23**	**-0.42**	**-0.18**	**-0.12**		**0.50**	**-0.25**		**-0.07**	**0.24**
River Alluvium average									3.4		-0.23	25		0.22
2SD (n = 3)									1.5		0.12	5		0.08
Rocks average			-0.14	-0.21	0.16	0.65	0.15	-0.39	4.2	-0.19		27	-0.16	0.21
2SD (n = 4)			0.27	0.11	0.20	0.24	0.60	0.18	1.3	0.15		13	0.22	0.04

[1] Raw data for tau calculations tabulated in electronic appendix, including alluvium values used.

[2] Tau values also calculated for analysed rocks relative to alluvium to illustrate impact of choice of rock versus alluvium as "parent" material.

[3] 2 sigma uncertainties for $\delta^{65}Cu$ and $\delta^{66}Zn$ are 0.09 and 0.07 respectively, based on long-term reproducibility of standards.

342 **4. Results**

343 **4.1 Glen Feshie chronosequence: soils, alluvium, plants and water samples**

344 Cu and Zn concentrations and isotope data for the Glen Feshie soil chronosequence, as well as
345 relevant tau data, are given in Table 1. Table 1 also presents data for averages of 3-4 analyses each
346 of river alluvium and rock samples. The full major and trace element data required for the tau
347 calculations in Table 1 can be found in the electronic appendix.
348
349 Selected tau values as well as Cu and Zn isotope data for the four analysed soil profiles from Glen
350 Feshie are displayed in Figure 3. As noted previously, we use river alluvium as a reference parent
351 material. Tau calculation for rocks (Table 1) relative to river alluvium yield data that are generally
352 within ±0.2 of zero, suggesting that for many elements this choice is not critical. The exceptions are
353 Mn, where river alluvium is about 65% depleted over Nb relative to the rocks analysed, and Pb,
354 where river alluvium is about 40% depleted over Nb relative to rocks. Our choice of river alluvium
355 to calculate tau values is also justified by the fact that calculated taus for Na, Al, Fe and Mn are
356 close to zero for the C horizons in the younger soil profiles.
357
358 The fact that these young soils, developed on a granitoid substrate in a cold climate, display only
359 incipient weathering is demonstrated by the tau values for base cations like Na (contrast with older
360 soils developed on more rapidly weathering basaltic substrates in Figures 4-6) which are generally
361 only slightly less than zero in the upper soil horizons, and approach zero in the C horizons. Al and
362 Fe are relatively depleted in the upper horizons of the 1-13 kyr soil profiles, and variably enriched
363 in the B horizons, suggesting translocation downwards, perhaps in association with organic acids
364 (e.g. Bigalke et al., 2011). Mn is slightly enriched relative to Nb throughout the youngest profile but
365 is depleted throughout all other soil profiles except the B horizon in the 3.6 kyr soil. Absolute Mn
366 enrichments or depletions depend critically, however, on whether river alluvium or rock
367 concentration values are used as a reference. Phosphorous concentrations (Fig. 3) show an evolution
368 through the chronosequence. This element is only depleted in the deepest horizons of the oldest soil
369 profile. In the two youngest soils it is depleted in the upper horizons whereas it is strongly enriched
370 at the top of the two oldest profiles. A final feature is a strong enrichment in Pb (Table 1, not
371 figured) in the H horizons of the two oldest profiles.

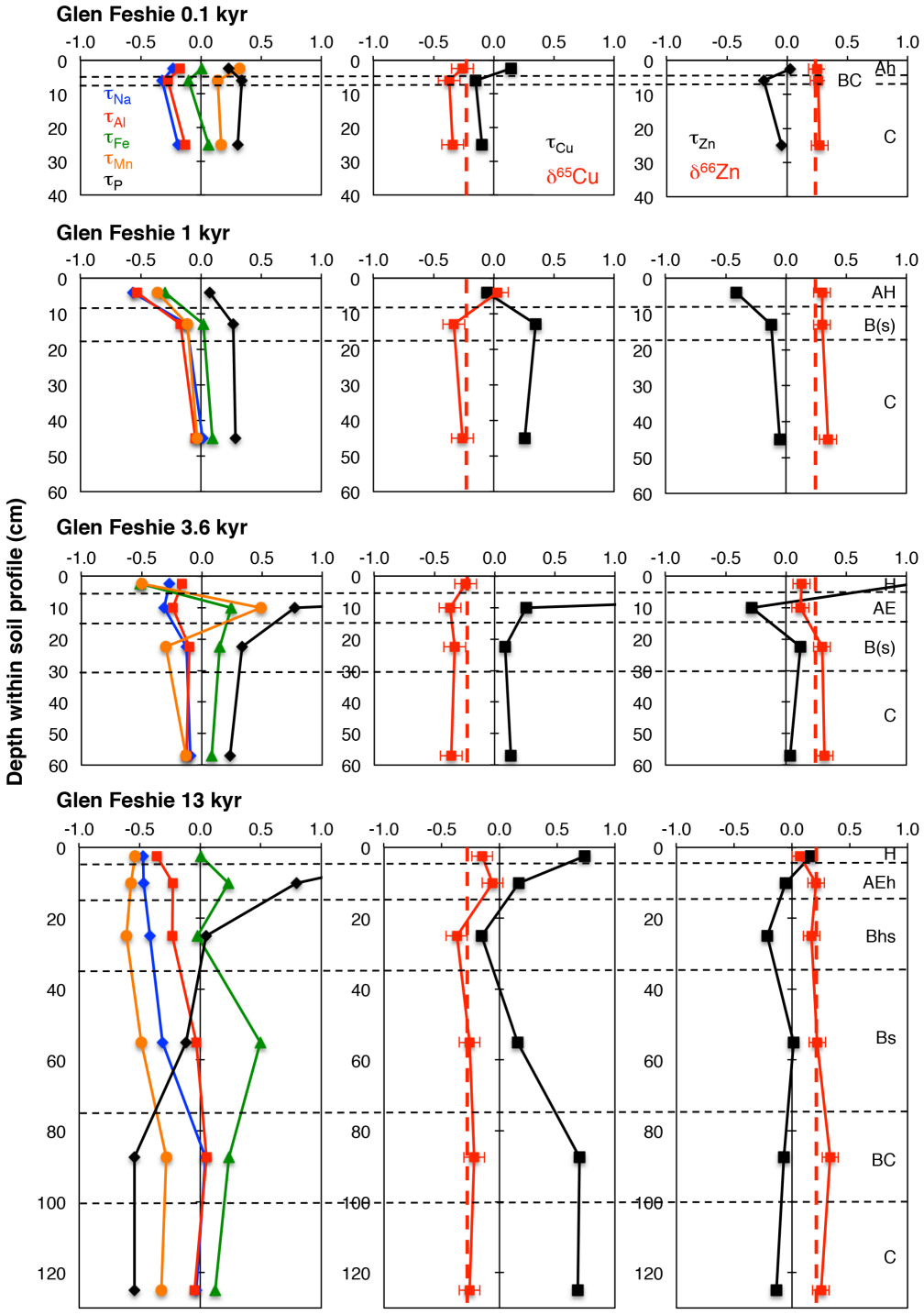

Figure 3: Tau parameters for selected elements (left), τ (black) and isotope (red) data for Cu (centre) and Zn (right) in Glen Feshie soils. The y axis in all plots is drawn at τ = 0 to highlight gain or loss of each element. The red dashed lines in the panels at centre and right show the isotope composition of river alluvium (Table 1) to highlight shifts in isotope composition of the soil relative to this reference. Horizontal dashed lines show horizon boundaries.

Cu is nearly always enriched in these soils, relative to the starting material. Though this could again be an artefact of the initial concentrations used to calculate taus, the data in Table 1 suggest that this picture would also emerge if local rocks were used as a reference. Zn, in contrast, is almost always

depleted. The tau profiles do, however, suggest significant translocation of Cu and Zn during incipient weathering. The most fully developed soil profiles (3.6 and 13 kyr) show enrichments in Cu and Zn near the top, correlated with those in phosphorous (Fig. 3), while AE and B horizons are usually depleted relative to horizons above and below. These features of Cu and Zn distribution within the soils are reminiscent of those previously found for cambisols and podzols by Bigalke et al. (2011). Incipient weathering, and the translocations of Cu and Zn within the soil profiles, is associated with barely significant shifts in Cu and Zn isotopes (Fig. 3). Overall, Cu isotopes are very slightly heavier (0.07-0.26‰ heavier than the profile average, and in the case of the 13 kyr soil heavier than the starting material) at the top of each profile and very slightly light (up to 0.12‰ lighter than the profile average) lower down. If anything there is a subtle change downwards in Zn isotopes towards slightly heavier (e.g. by 0.26‰ in the 13 kyr soil) isotope compositions.

Table 2: Cu and Zn concentration and isotope data for river water and plants from Glen Feshie.

Sample	Type	Soil age (kyr)	[Cu] ppm	$\delta^{65}Cu$[1]	[Zn] ppm	$\delta^{66}Zn$
GFP1	Heather - leaves	1	4.0	-0.84	0.59	-0.40
GFP2	Heather - roots	1	2.1	-1.02	0.36	0.00
GFP3	Heather - leaves	13	6.6	-0.35	0.73	-0.45
GFP4	Heather - stems	13	2.0	-0.79	0.21	-0.30
GFP5	Heather - roots	13	2.1	-0.80	0.46	-0.17
GFP6	Grass	13	4.7	-0.22	1.39	0.01
			[Cu] nM	**$\delta^{65}Cu$**	**[Zn] nM**	**$\delta^{66}Zn$**
GFWn1	River water		2.7	0.01	17	0.50
GFWn4	River water		4.0	-0.04	12	0.48
GFWn6	River water		1.9	0.13	14	0.55
GFWn7	River water		3.8	0.11	19	0.53
GFWn8	River water		5.0	-0.07	22	0.40

[1] 2 sigma uncertainties for $\delta^{65}Cu$ and $\delta^{66}Zn$ are 0.09 and 0.07 respectively, based on long-term reproducibility of standards.

Cu and Zn abundance and isotope data for plants and river water collected in Glen Feshie are presented in Table 2. Concentrations of Cu in the River Feshie are low, ranging from 1.9 to 5.0 nM and consistent with the low concentrations seen in other relatively undisturbed catchments like the Kalix (northern Sweden) and the Amazon (Vance et al., 2008). Zn concentrations range from 12-22 nM, again within the range of values for the Kalix and Amazon (Little et al., 2014a). $\delta^{65}Cu$ in the River Feshie samples are -0.07 to +0.13‰, compared to a wide range of +0.02 to +1.45 in global

405 rivers (Vance et al., 2008). In common with these previous data, the Feshie is about 0.2-0.3‰
406 heavier than the soils it drains and the river alluvium it carries (Vance et al., 2008). δ^{66}Zn is +0.40
407 to +0.55‰, also heavier than the solid material the river carries (at +0.22‰).
408
409 The plant samples are all isotopically lighter for Cu and Zn than the soils on which they grow, with
410 δ^{65}Cu ranging from -0.22 to -1.02 and δ^{66}Zn from +0.01 to -0.45‰. Plant samples contain 2.0-6.6
411 ppm Cu, in the same range as previously observed (e.g. Weinstein et al., 2011). Zn contents in the
412 plants are 1-2 orders of magnitude lower than previously observed (Weiss et al., 2005; Viers et al.,
413 2007; Arnold et al., 2010), at 0.2-1.4 ppm Zn. Our purpose in presenting the plant data is to
414 facilitate a later discussion of their impact on soil development. It is not to present a detailed
415 discussion of the mechanisms of Cu and Zn uptake by plants, which has recently been reviewed
416 (Moynier et al., 2016). All plants yet studied have a bulk Cu isotopic composition lighter than the
417 external pool (e.g. Weinstein et al., 2011) while for Zn bulk plants can be both heavier and lighter
418 than this pool, depending on whether free or complexed Zn is taken up (e.g. Weiss et al., 2005;
419 Arnold et al., 2010).

Table 3: Mass balance (τ) calculations, Cu and Zn concentration and isotope data, for Hawaiian soils.

Sample	Horizon	Depth (cm)	τ_{Ca}[1]	τ_{Al}	τ_{Fe}	τ_{Mn}	τ_{P}	τ_{Pb}	[Cu] ppm	τ_{Cu}	$\delta^{65}Cu$[2]	[Zn] ppm	τ_{Zn}	$\delta^{66}Zn$
Ola,a, Kilauea, 0.3 kyr, 2500 mm														
Ola'a A	Oe+Oa	0-8	-0.10	0.02	-0.01	-0.13	0.04	1.40	97	-0.04	0.05	108	0.15	0.30
Ola'a B	Oa	8-13	-0.17	-0.02	-0.03	-0.19	0.01	1.48	84	-0.22	0.01	104	0.03	0.26
Ola'a C	A	13-21	-0.12	-0.08	-0.02	-0.24	-0.17	0.35	94	-0.16	0.07	117	0.10	0.31
Ola'a D	Bw	21-27	-0.08	-0.05	0.03	-0.21	-0.31	-0.11	113	-0.02	0.09	100	-0.07	0.34
Ola'a E	C1	27-38	-0.05	-0.07	0.02	-0.20	-0.31	-0.14	117	0.03	0.12	106	-0.01	0.32
Ola'a F	C2	38-49	0.03	0.05	0.00	-0.23	-0.29	0.36	114	0.00	0.00	109	0.02	0.38
Ola'a G	C3	49-73	0.05	0.03	0.01	-0.21	-0.31	0.29	117	0.02	0.14	115	0.07	0.33
Integrated			**-0.01**	**0.00**	**0.01**	**-0.21**	**-0.27**	**0.28**		**-0.01**	**0.10**		**0.04**	**0.33**
Laupahoehoe, Mauna Kea, 20 kyr, 2500 mm														
LA 10	Oe	0-5	-0.99	-0.18	-0.12	-0.76	-0.32	0.55	32	0.45	0.25	39	-0.80	0.32
LA 6	Oa	5-12	-0.99	-0.56	-0.52	-0.80	-0.54	-0.20	27	-0.32	0.30	80	-0.77	0.38
LA 11	A	12-20	-0.99	-0.85	-0.51	-0.92	-0.56	0.13	23	0.13	-0.35	49	-0.73	0.38
LA 7	A	20-27	-1.00	-0.91	-0.44	-0.90	-0.84	-0.24	14	-0.79	-0.60	104	-0.82	0.24
LA 12	Bw1	27-39	-0.99	-0.81	-0.22	-0.88	-0.75	0.03	16	-0.64	-0.48	73	-0.82	0.31
LA 8	Bw2	39-52	-0.99	-0.64	-0.50	-0.82	-0.68	-0.43	10	-0.76	0.04	91	-0.77	0.39
LA 13	Bw3	52-71	-1.00	-0.76	-0.35	-0.86	-0.73	-0.20	13	-0.73	-0.19	91	-0.78	0.41
LA 9	Bw3+Bw4	71-94	-0.98	0.03	-0.24	-0.68	-0.33	-0.18	20	0.04	-0.04	46	-0.74	0.27
LA 14	Bw4	94-103	-0.98	-0.14	-0.32	-0.72	-0.42	-0.11	26	0.22	0.05	51	-0.73	0.36
Integrated			**-0.99**	**-0.43**	**-0.34**	**-0.79**	**-0.55**	**-0.16**		**-0.29**	**-0.08**		**-0.76**	**0.35**
Kohala, Hawi, 150 kyr, 2500 mm														
KoM 7	Oe+A1	0-12	-0.98	-0.72	-0.08	0.25	-0.52	2.74	38	0.92	-0.07	138	-0.33	0.46
KoM 8	A1+A2	12-21	-0.99	-0.73	0.15	-0.07	-0.69	2.60	15	-0.41	0.00	99	-0.63	0.30
KoM 9	A2+2Bw1	21-27	-0.96	-0.59	0.58	0.05	-0.77	1.82	12	-0.49	0.15	95	-0.61	0.34
KoM 10	3Bw2	27-39	-0.99	-0.40	0.49	-0.09	-0.73	2.42	15	-0.22	0.18	73	-0.63	0.44
KoM 11	3Bw3	39-51	-0.99	-0.26	0.23	0.03	-0.73	1.52	21	-0.01	0.38	88	-0.60	0.40
KoM 12	3Bw3	51+	-0.99	-0.25	-0.01	0.16	-0.58	0.88	22	-0.19	0.26	91	-0.68	0.81
Integrated			**-0.98**	**-0.45**	**0.22**	**0.04**	**-0.67**	**1.94**		**-0.09**	**0.13**		**-0.60**	**0.43**

Table 3 (continued): Mass balance (τ) calculations, Cu and Zn concentration and isotope data, for Hawaiian soils

Sample	Horizon	Depth (cm)	τ_{Ca}[1]	τ_{Al}	τ_{Fe}	τ_{Mn}	τ_{P}	τ_{Pb}	[Cu] ppm	τ_{Cu}	$\delta^{65}Cu$[2]	[Zn] ppm	τ_{Zn}	$\delta^{66}Zn$
Kohala H, Hawi, 150kyr, 1060 mm														
KOH-1	Ap	0-22	-0.73	0.16	0.06	5.03	-0.27	1.65	28	1.05	-0.18	135	-0.05	0.43
KOH-2	Bw1	22-31	-0.83	-0.01	-0.11	2.55	-0.66	0.79	14	-0.27	-0.03	113	-0.44	0.28
KOH-3	Bw1+Bw2	31-41	-0.82	0.06	0.01	2.47	-0.62	0.51	10	-0.48	0.56	107	-0.47	0.24
KOH-4	Bw2	41-51	-0.76	0.03	0.03	2.59	-0.33	0.14	5.2	-0.73	0.36	102	-0.49	0.29
KOH-5	Bw2+Bw3	51-59	-0.79	0.02	0.04	2.08	-0.49	0.13	5.8	-0.68	0.92	107	-0.43	0.33
KOH-6	Bw3	59+	-0.79	0.01	0.05	1.86	-0.48	0.11	4.9	-0.73	0.89	84	-0.56	0.49
Integrated			**-0.78**	**0.07**	**0.02**	**3.14**	**-0.44**	**0.74**		**-0.08**	**0.06**		**-0.35**	**0.36**
Maui Climosequence, Site 2, 400kyr, 2450 mm														
2A1	A	0-5	-0.98	-0.87	-0.35	-0.70	-0.79	0.90	30	-0.51	-0.40	114	-0.54	0.37
2A2	Ag	5-12	-0.99	-0.88	-0.33	-0.77	-0.87	0.79	33	-0.63	-0.61	128	-0.64	0.32
2A3	Bw1	12-24	-1.00	-0.87	-0.21	-0.86	-0.92	1.12	15	-0.85	-0.42	70	-0.82	0.33
2A4	Bw2	24-34	-1.00	-0.83	-0.21	-0.89	-0.91	0.82	10	-0.90	-0.56	54	-0.87	0.27
2A5	Bg	34-55	-1.00	-0.81	-0.44	-0.86	-0.93	1.16	18	-0.83	-0.49	84	-0.81	0.33
2A6	Bw3	55-69	-1.00	-0.82	-0.42	-0.89	-0.92	0.87	17	-0.85	-1.09	83	-0.82	0.28
2A7	Bw4	69-100	-1.00	-0.70	-0.28	-0.87	-0.84	0.60	13	-0.85	-0.80	66	-0.80	0.29
Integrated			**-1.00**	**-0.81**	**-0.33**	**-0.86**	**-0.89**	**0.90**		**-0.82**	**-0.67**		**-0.79**	**0.31**
Maui Climosequence, Site 4, 400kyr, 3350 mm														
4A2	A2	3-10	-1.00	-0.84	-0.79	-0.96	-0.74	0.87	6.0	-0.95	-0.01	37	-0.92	0.40
4A3	Bg	10-17	-1.00	-0.87	-0.85	-0.96	-0.76	2.02	8.8	-0.93	-0.02	41	-0.92	0.36
4A4	Bw1	17-21	-1.00	-0.89	-0.88	-0.97	-0.92	0.91	5.8	-0.97	-0.10	44	-0.94	0.39
4A5	Bw2	21-34	-1.00	-0.88	-0.85	-0.97	-0.94	0.90	5.8	-0.97	-0.28	51	-0.94	0.36
4A6	Bw3	34-51	-1.00	-0.89	-0.85	-0.96	-0.94	0.89	5.3	-0.97	-0.24	39	-0.94	0.40
4A7	Bw4	51-75	-1.00	-0.66	-0.83	-0.97	-0.79	0.58	5.1	-0.96	0.10	34	-0.93	0.39
Integrated			**-1.00**	**-0.78**	**-0.84**	**-0.97**	**-0.86**	**0.75**		**-0.96**	**-0.06**		**-0.93**	**0.38**

Table 3 (continued): Mass balance (τ) calculations, Cu and Zn concentration and isotope data, for Hawaiian soils

Sample	Horizon	Depth (cm)	τ_{Ca}[1]	τ_{Al}	τ_{Fe}	τ_{Mn}	τ_{P}	τ_{Pb}	[Cu] ppm	τ_{Cu}	$\delta^{65}Cu$[2]	[Zn] ppm	τ_{Zn}	$\delta^{66}Zn$
Maui Climosequence, Site 6, 400kyr, 5050 mm														
6A1	Ag1	0-14	-0.87	-0.78	-0.88	-0.84	0.00	5.03	5.2	-0.36	-0.01	23	-0.30	0.59
6A2	Ag2	14-26	-1.00	-0.88	-0.97	-0.97	-0.90	2.06	5.3	-0.96	-0.56	20	-0.96	0.63
6A3	Bg1	26-38	-1.00	-0.84	-0.97	-0.97	-0.90	2.08	11	-0.88	-0.63	16	-0.96	0.56
6A4	Bg2	38-49	-1.00	-0.92	-0.98	-0.96	-0.97	0.88	4.7	-0.98	-0.13	26	-0.98	0.42
6A5	Bg3	49-67	-1.00	-0.94	-0.98	-0.97	-0.98	0.71	2.8	-0.99	-0.09	30	-0.98	0.46
6A6	Bg4	67-93	-1.00	-0.76	-0.97	-0.97	-0.86	-0.01	2.6	-0.98	-0.01	26	-0.96	0.26
Integrated			**-0.98**	**-0.86**	**-0.96**	**-0.95**	**-0.81**	**1.51**		**-0.89**	**-0.32**		**-0.88**	**0.45**

[1] Raw data for tau calculations tabulated in electronic appendix, including parent rock values used.

[2] 2 sigma uncertainties for $\delta^{65}Cu$ and $\delta^{66}Zn$ are 0.09 and 0.07 respectively, based on long-term reproducibility of standards.

433 **4.2 Basaltic Soil Development, Hawaiian Islands**

434 Cu and Zn concentrations and isotope data for all the Hawaiian soils, as well as relevant tau data,
435 are given in Table 3. The full major and trace element data required for the tau calculations in Table
436 3, including data used to represent parent material, can be found in the electronic appendix.
437
438 Selected tau values as well as Cu and Zn isotope data for the three analysed soil profiles from the
439 LSAG chronosequence are displayed in Figure 4. As expected, chemical and isotopic features
440 associated with weathering processes are clearer in these data than at Glen Feshie, in older soils,
441 developed on more rapidly weathering basaltic substrates, in a setting with significantly higher
442 annual rainfall. However, there are also complications introduced by mineral aerosol addition that
443 become evident at the older end of the chronosequence.
444
445 In the youngest soil profile at Ola'a Kilauea (0.3 kyr, Fig. 4) only Mn and P are substantially
446 depleted relative to Nb. The 20 kyr profile at Laupahoehoe, Mauna Kea, in contrast, shows near
447 total depletion of base cations (e.g. Ca, Fig. 4) and moderate depletion of Fe, while ~90% of the
448 original Mn has been lost from the profile. Aluminium and phosphate show similar patterns to each
449 other, with marked depletions in most of the B horizon and only slight depletions in the O horizons
450 and the lowest part of the profile studied. At the 150 kyr site the maximum enrichment in Fe at 20-
451 30 cm correlates with a peak in quartz+mica abundances (Kurtz et al., 2001). Moreover, Pb
452 enrichment throughout this profile (Table 3, not figured) has previously been attributed to aeolian
453 dust deposition on the basis of its isotopic composition (Monastra et al., 2004). It seems likely that
454 the lack of Mn depletion compared to the younger Laupahoehoe profile is also attributable to dust
455 deposition.
456
457 The 300 year old, Ola'a soil exhibits only small shifts in abundance or isotopic patterns compared
458 to parent rock values. The slight depletion in the A and upper B horizons develops into a more
459 pronounced feature with soil age in the Laupahoehoe and Kohala M profiles. At Laupahoehoe this
460 Cu depletion is associated with an isotopic fractionation, such that the most depleted upper B
461 horizon has a δ^{65}Cu about 0.7 ‰ lighter than the starting material. The minimum in δ^{65}Cu and the
462 maximum Cu depletion occurs around the break in the profile noted earlier (see dashed blue line in
463 Fig. 4). The lower B horizon is identical to the starting material while the O horizon is about 0.2 ‰
464 heavier. In contrast, Zn becomes uniformly depleted throughout the Laupahoehoe profile, with 75-
465 80% of the original inventory lost from the soil. Moreover, this loss is associated with barely

significant isotopic effects. Cu and Zn in the older Kohala M profile are again more complicated, perhaps also due to dust deposition. Depletions in Cu and Zn are less intense than at Laupahoehoe, and there has been net addition of Cu to the top of the profile. Cu isotopes shifts from the parent material (at about +0.2 ‰ relative to parent material) are only significant at the bottom of the profile, where Zn is also heavy (+0.5‰ relative to starting material).

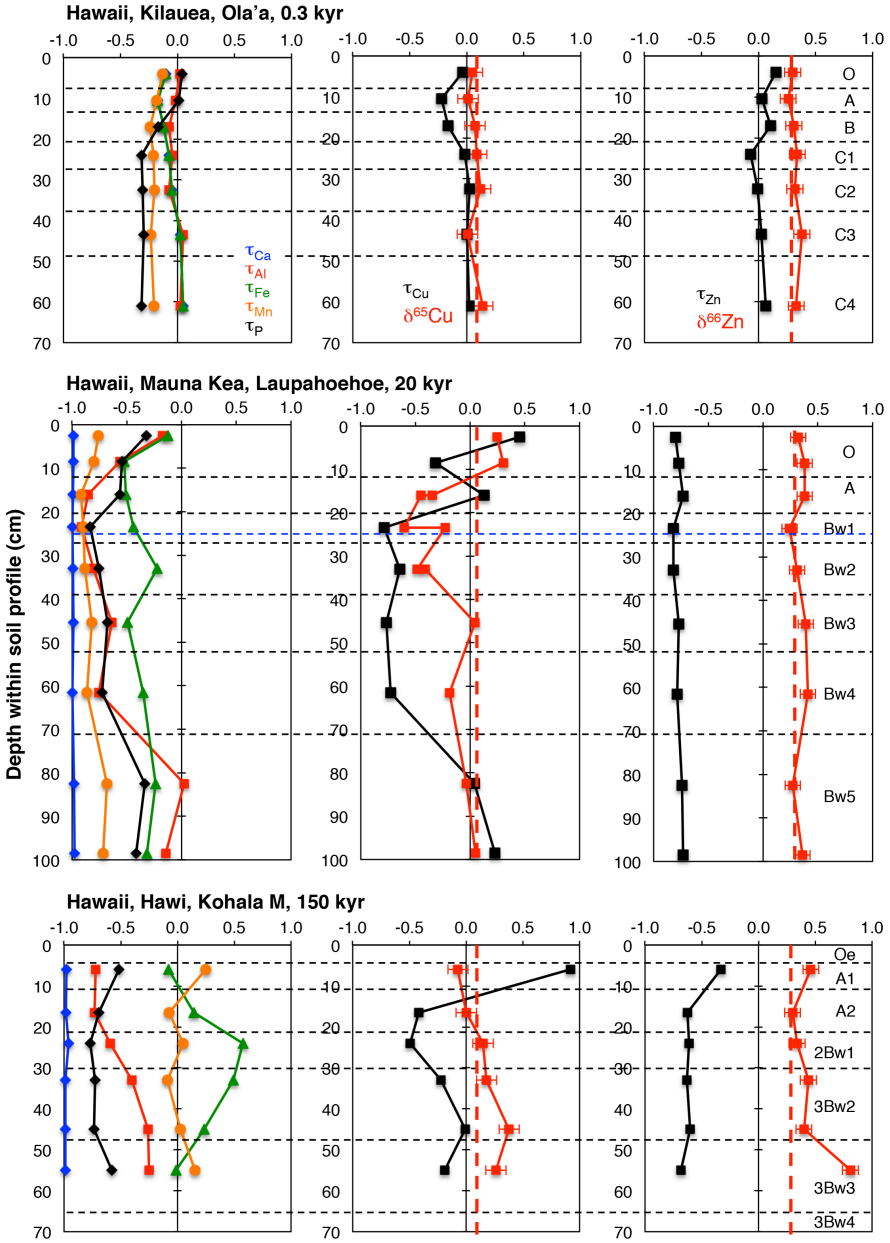

Figure 4: Tau parameters for selected elements (left), τ (black) and isotope (red) data for Cu (centre) and Zn (right) in LSAG soils, island of Hawaii. The y axis in all plots is drawn at τ = 0 to highlight gain or loss of each element. The horizontal dashed blue line in the Laupahoehoe panels marks the break in this profile between the 5 kyr ash on top and the 20kyr tephra below. The red dashed lines in the panels at centre and right show the isotope composition of parent basalt to highlight shifts in isotope composition of the soil relative to this reference. The reference value for Cu is the average for all ocean island basalts in Liu et al. (2015), for which $\delta^{65}Cu = +0.09 \pm 0.07$ (1SD). That for Zn is the average for Kilauean basalts in Chen et al. (2013), for which $\delta^{66}Zn = +0.29 \pm 0.03$ (1SD). Horizontal dashed lines show horizon boundaries.

There are some striking differences between the two 150 kyr sites at Kohala that receive different annual rainfall – as well as some intriguing similarities. The lower rainfall site (Kohala H, 1060 mm), shows pronounced Mn enrichment that peaks in the upper part of the profile (Fig. 5). Base cations (e.g. Ca in Fig. 5) and P show lesser depletion than at Kohala M, while Fe and Al are barely depleted at all. In contrast to the rather different mass balance behaviours for these major elements, Cu and Zn show rather similar patterns at the two sites, both in their mass balance and isotopic compositions. Thus both sites show large enrichments of Cu at the top of the profile, in the case of the Kohala H profile closely co-incident with the peak in Mn enrichment. Both profiles show a change in δ^{65}Cu from values around 0.2-0.3 ‰ lighter than parent material at the top, to values distinctly heavier at the bottom, though this is much more pronounced at Kohala H. Zn is about 70-80% depleted throughout both profiles, with the exception of the upper horizon where depletions are distinctly lower, again especially at Kohala H. Zn isotopes also show the same pattern, with values very close to parent material in the upper B horizon contrasting with significantly heavier values above and below, in this case more pronounced at Kohala M.

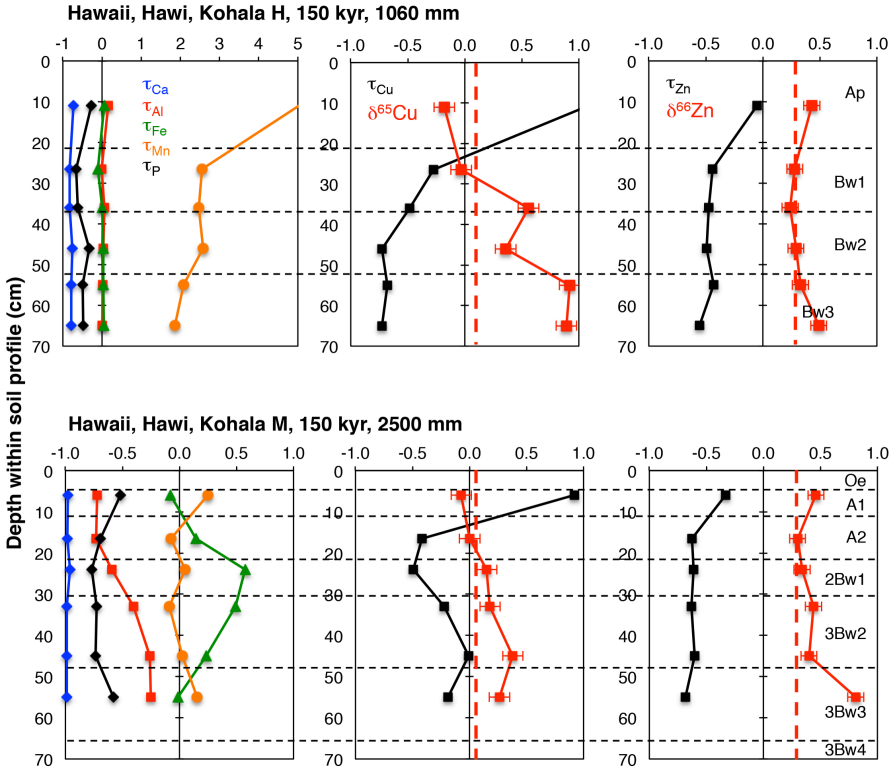

Figure 5: Tau parameters for selected elements (left), τ (black) and isotope (red) data for Cu (centre) and Zn (right) in Kohala soils, island of Hawaii. The y axis in all plots is drawn at τ = 0 to highlight gain or loss of each element. Note the different scale on the tau plot for Kohala H. The red dashed lines in the panels at centre and right show the isotope composition of parent basalt (electronic appendix) to highlight shifts in isotope composition of the soil relative to this reference. Reference isotope values from same source as in Fig. 4.

4.3 Maui rainfall gradient: influence of climate on Cu and Zn Distributions

Selected tau values as well as Cu and Zn isotope data for the three analysed soil profiles from the Maui rainfall gradient are displayed in Figure 6. Base cations and aluminium are all very strongly depleted in these soils, and the main feature visible in the tau data on Fig. 6 is the drop in Fe concentrations between annual rainfall values of 2500mm and 3350 mm (sites 2 and 4 on Fig. 6) as a result of the change in redox state that has been noted in previous publications (Schuur et al., 2001; Chadwick and Chorover, 2001; Miller et al., 2001; Scribner et al. 2006), caused by a transition from well-drained to water-logged soils as rainfall increases.

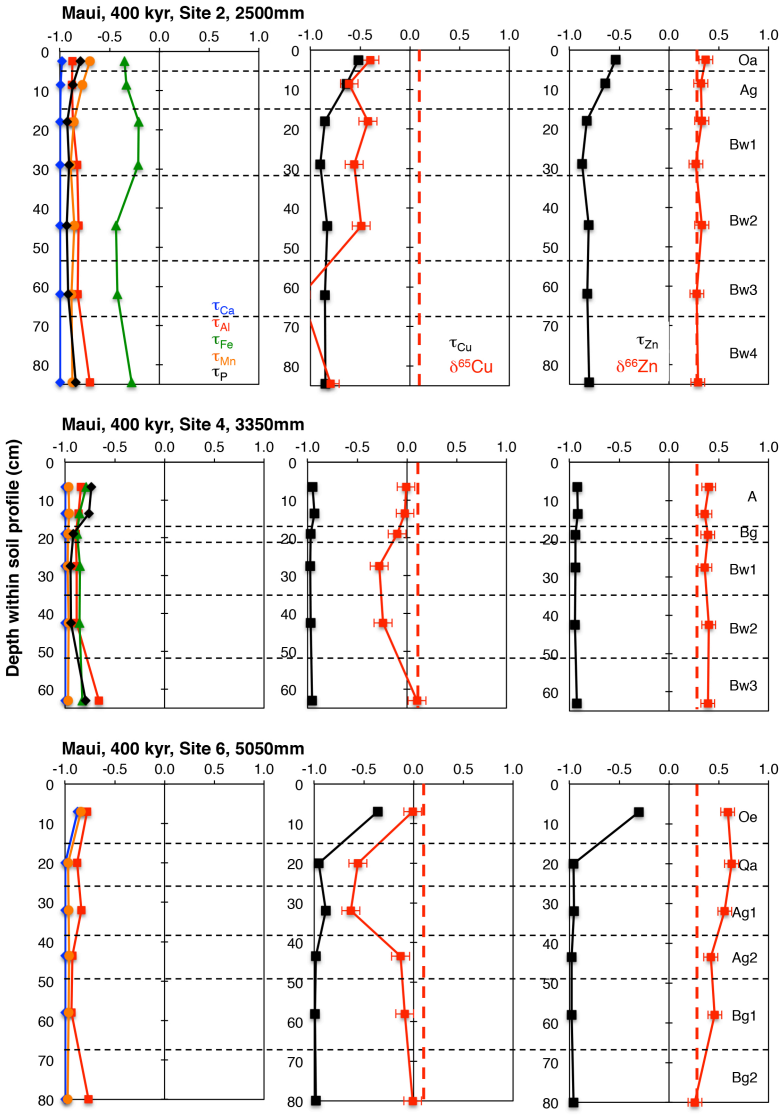

Figure 6: Tau parameters for selected elements (left), τ (black) and isotope (red) data for Cu (centre) and Zn (right) in Maui soils. The y axis in all plots is drawn at τ = 0 to highlight gain or loss of each element. The red dashed lines in the panels at centre and right show the isotope composition of parent basalt (electronic appendix) to highlight shifts in isotope composition of the soil relative to this reference.

The disappearance of Fe oxides along the rainfall gradient is associated with changes in the behaviour of Cu and Zn and their isotopes (Fig. 6). The 2500mm site, which retains some Fe in secondary oxyhydroxide phases (Schuur et al., 2001; Chadwick and Chorover, 2001; Miller et al., 2001; Scribner et al. 2006) has the lightest Cu isotopes measured in this study, with δ^{65}Cu up to 1.2 ‰ lighter than parent material. This profile also retains the most Cu of the three Maui sites, with τ_{Cu} values suggesting loss of 50-90% of the initial inventory. In contrast, Cu loss at the other two sites is nearly complete, except in the Oe horizon of Site 6 (5050mm rainfall). Moreover, though the intermediate depths of the two wetter profiles retain the light Cu isotope signature, with δ^{65}Cu at 0.3-0.7‰ lighter than parent material, this is bracketed by much heavier isotope compositions (<0.1‰ lighter than the parent isotope composition) at top and bottom. τ_{Zn} shows patterns at these three sites that are very similar to τ_{Cu}: strong depletion throughout but less strong at Site 2 and moderate at the top of Site 6. Zn isotopes again show rather subtle shifts from parent material values: no shift at all at site 2 and increasing shifts across the rainfall/redox gradient, culminating in δ^{66}Zn ~0.35‰ heavier than parent material in the O horizon of the wettest Site 6.

5. Discussion

Our overall objective in this contribution is to assess the extent to which processes in soils can explain the characteristics of Cu and Zn isotopes in the dissolved phase of rivers. Though Cu isotope compositions in the incipient weathering environment of Glen Feshie document a dissolved riverine pool that is only marginally heavier than alluvium and soils (-0.07 to +0.11‰ versus -0.23‰), Vance et al. (2008) found that large rivers globally were universally heavier than continental crust, at δ^{65}Cu = +0.02 to +1.45‰ with a discharge weighted average of +0.68‰, much heavier than the bulk continental crust at around 0 to +0.2‰. The same study found that particulate-associated Cu in one small river was 1.2±0.4‰ lighter than the dissolved phase. Zn isotopes in large and small rivers (Little et al., 2014a), though likely more severely impacted by anthropogenic activities (e.g. Chen et al., 2008), display much more subtle variations and the global dissolved riverine flux to the oceans is identical to the upper continental crust at +0.33‰ (Little et al., 2014a).

In pursuing this objective, however, complications arise due to a suite of pedological processes that overprint the impact of chemical weathering, such as variability in redox conditions, addition of mineral aerosol, and biological redistribution of elements. In the following we attempt to pick apart the datasets presented here to try to understand the impact of each of these processes individually before concluding with an assessment of the degree to which soils lose heavy or light Cu and Zn

isotopes during the weathering process. We acknowledge that this approach, of isolating a single dominant controlling process in each profile, simplifies somewhat. Given the multiplicity and complexity of soil processes, however, it is a more instructive analytical approach than an attempt to consider all the contributing processes in each soil profile.

5.1 Cu-Zn loss and redox processes in the Maui rainfall sequence

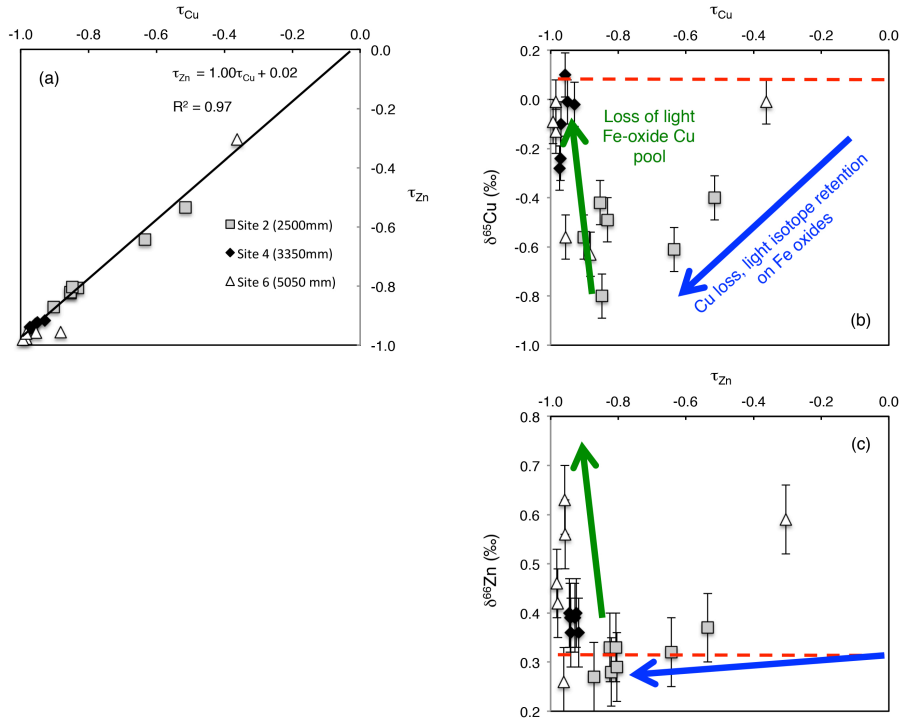

Figure 7: τ_{Cu}, τ_{Zn} and Cu and Zn isotope compositions in Maui soils. Cu and Zn are clearly lost from the parent material of these soils in proportions very closely related to their original concentrations. In the 2500mm, oxic, soil this is associated with the loss of the heavy isotope of Cu, and a very subtle fractionation of Zn in the same direction (blue arrows), probably controlled by partitioning of isotopes between aqueous organic complexes and Fe oxides retained in the soil. In the wetter, reducing, soils, however, the dominant process involves a move to heavy isotope compositions and the near total depletion of Cu and Zn. We suggest that this is due to the well-known loss of the Fe oxide pool in these anaerobic, water-logged soils (e.g. Schuur et al., 2001; Scribner et al., 2006; Thompson et al., 2011), leaving a residual pool of Cu that is close to the original rock composition (red dashed lines in (b) and (c)) and of Zn that is significantly heavier than the original parent material.

In many ways the Maui rainfall sequence presents the clearest set of processes seen in this study. This is emphasized by the data presented in Figure 7, which plots τ_{Cu} versus τ_{Zn}, $\delta^{65}Cu$ and $\delta^{66}Zn$ for this set of soils. The data in Figure 7a demonstrate that Zn and Cu behave remarkably coherently in these soil samples, being lost in precise proportion to their original concentrations in parent material, as illustrated by the line fitted to all the data but effectively defined by data from Site 2. Soil samples from the two more reduced sites plot at the lower left end of the array, having lost almost all their Cu and Zn, with the exception of the topmost sample from Site 6. Cu-Zn data from these sites show no relationship with quartz contents, which peak at 18-22 wt % in the upper

levels of Sites 2 and 4 (Scribner et al., 2006), but it nevertheless seems likely that the higher Cu and Zn concentrations at the uppermost horizon of Site 6 is due to some kind of addition at the surface. Though there is no overall correlation between τ_{Pb} and Cu and Zn abundances in these soils, τ_{Pb} is higher in this sample than any other (at 5.03, Table 3), and it is possible that the added Cu and Zn is anthropogenic in origin as opposed to mineral aerosol.

Aside from this sample, data for Cu and Zn isotopes also behave in a relatively straightforward way at these sites (Fig. 7b, c). At Site 2 progressive Cu depletion is clearly associated with preferential loss of isotopically heavy Cu, or retention of light Cu, such that the most Cu-depleted soils in the B horizon at Site 2 (85-90% loss) have δ^{65}Cu as low as -1.09‰. At the other two sites where, aside from the exceptional sample at the top of Site 6 mentioned above, Cu loss becomes extreme (up to 99%) and the isotopic composition of this small residual pool shifts back towards the isotopic composition of the parent material (red dashed line in Fig. 7b). The pattern for Zn isotopes is similar except that the shift to light isotopes upon Zn loss is very subtle while the shift to heavier isotopes at Sites 4 and 6 takes the residual Zn beyond the initial parent material to δ^{66}Zn that is up to 0.35‰ heavier.

While there may be a number of potential explanations for the patterns in Fig. 7, they are consistent with some observations that have been made before in soils (e.g. Bigalke et al., 2010a, 2011), and are also consistent with a dual set of processes that are both controlled by the redox switch in the middle of this rainfall sequence (Schuur et al., 2001). Though none of the Maui soils are podzols (van Breemen and Buurman, 2004), there has clearly been translocation of Fe and Al through and out of the soil (Fig. 6). The aqueous organic species that complex Fe also complex Cu and Zn (e.g. Grybos et al., 2007; Bigalke et al., 2010b; Ryan et al., 2014) and move them through and out of the soil as well (e.g. Keller and Domergue, 1996; Bigalke et al., 2010a,b, 2011). In contrast, sorption of both Cu and Zn to Fe-Mn oxyhdyroxides tends to retain both elements in soils, and the trace metal characteristics of soils have been described in terms of the dual controls of mobile aqueous organic species and oxyhydroxide surfaces (e.g. Grybos et al., 2007). We suggest that it is these two competing processes that determine the patterns in Fig. 7, with heavy Cu and slightly heavy Zn moved out of the soil complexed to aqueous organic species. The light Cu, and very slightly light Zn, retained in the dry soil at Site 2, we suggest, is sorbed to Fe oxide phases (blue arrows on Fig. 7). At the high rainfall end of the gradient, Fe-oxides are lost by reduction and with them the light Cu and Zn, leaving a very small residual pool that is isotopically similar to the parent material for Cu, and distinctly heavier for Zn (green arrows in Fig. 7). We note that though conditions are

609 reducing enough in the two wetter soils to mobilise Fe as Fe(II), there is no evidence that they are
610 reducing enough to form sulphide. The measured Eh at Site 4 where the Fe oxides first disappear is
611 about +300 mV, at Site 6 it is around zero (Schuur et al., 2001). It is possible that wet periods and
612 occasional water-logging could cause Eh to descend transiently from the above measured values,
613 closer to that for sulphate reduction. However, even in water-logged floodplain soils that can
614 become anoxic enough to encounter sulphate reduction, trace metal mobility is controlled by release
615 from Fe oxyhydroxides, organic matter or mobilisation of colloidal metal forms (e.g. Grybos et al.,
616 2007; Weber et al. 2009, 2010).
617
618 There is experimental and theoretical support for this scenario (reviewed in detail in Moynier et al.,
619 2016), and natural Cu-Zn isotopic data for rivers and the oceans (Vance et al., 2008; Little et al.,
620 2014a,b) suggest that these controls are ubiquitous in controlling partitioning of Cu and Zn isotopes
621 between aqueous and particulate phases at the Earth's surface. As summarised in a recent review
622 (Moynier et al., 2016), experimental studies of the sorption of Cu and Zn isotopes to Fe-Mn
623 oxyhydroxides suggest a range of behaviours. Thus, Pokrovsky et al. (2005) document small
624 (<0.2‰) Zn isotope fractionations, in both positive and negative directions depending on the
625 mineral phase, between inorganic aqueous species and sorption to oxides – in both directions
626 depending on identity of oxide and never more than ±0.2 per mil. Juillot et al. (2008) observed
627 preferential sorption of heavy Zn isotopes to ferrihydrite and goethite by 0.3-0.5‰ and Balistrieri et
628 al. (2008) found sorption of heavy Cu and Zn onto Fe oxyhydroxides, by 0.7 and 0.5‰
629 respectively. Some of this variability might be rationalised by the recent study of Bryan et al.
630 (2015), who found that sorption to Mn-oxide (birnessite) involved no significant fractionation at
631 low ionic strengths, whereas at ionic strengths equivalent to seawater sorption to birnessite strongly
632 favours the heavy isotope.
633
634 Sorption of residual metal to the solid, however, is only half the story. All the above experiments
635 were performed with reference to an aqueous phase in which the Cu and Zn were in simple
636 inorganic species. But these two metals are ubiquitously complexed to aqueous organic ligands in
637 natural solutions. These organic species have a strong preference for heavy metal isotopes due to
638 stiffer bonds (e.g. Fujii et al., 2014; see review in Moynier et al., 2016), and this often appears to
639 govern the distribution of their isotopes in nature (e.g. Little et al., 2014b). Experimentally, Jouvin
640 et al. (2009) and Bigalke et al. (2010b) document heavy isotopes of Zn and Cu associated with
641 humic acids, heavier than free aqueous ion by 0.25‰ in both cases. Most recently Ryan et al.
642 (2014) used a Donnan dialysis technique to show that ^{65}Cu is enriched over ^{63}Cu by +0.14 to

643 +0.84‰ in a range of soluble organic ligands relative to inorganic aqueous species, and that the size
644 of the fractionation was correlated with the stability constants of the complexes. We emphasise that
645 the organic species we invoke as important here transport Cu and Zn as organically-complexed
646 species in the aqueous phase. In our view this pool is removed from the soil, and will not be found
647 in residual organically-bound Cu and Zn that remains behind in soils and that is targeted through
648 sequential extractions studies (e.g. Kusonwiriyawong et al., 2016). This residual organic fraction
649 may be isotopically light if dominated by metabolic Cu and Zn from plants, or heavy if it has
650 undergone fractionation associated with solid-phase organic material such as humic acids.

651 We suggest that it is the mobilization of Cu and Zn into soil solutions that causes the extreme
652 depletion of Cu, and its heavy isotope, in the oxic site 2 soil profile at Maui, with residual light Cu
653 sorbed onto Fe oxyhydroxide surfaces. Cu isotope ratios in this profile are up to 1.1‰ lighter than
654 the parent material, however, either suggesting an organic complex with an even stronger
655 preference for the heavy isotope of Cu than documented by Ryan et al. (2014) or, perhaps more
656 likely, multiple cycles of Cu mobilization and re-adsorption to a smaller residual pool of Fe oxide in
657 a Rayleigh type process. In contrast to Cu, isotope effects during Zn depletion at Maui Site 2 are
658 very small (Fig. 7). This is consistent with the conclusion from the experimental data that Zn
659 isotopic partitioning between aqueous *organic* complexes and Fe-Mn oxyhydroxide surfaces must
660 be very small indeed. In this scenario, the shift towards heavy isotopes at the higher rainfall sites
661 would be explained by the removal of the isotopically light Fe oxide pool at the low redox
662 potentials observed (e.g. Schuur et al., 2001; Thompson et al., 2007). The fact that the residual pool
663 of Zn is heavier than the parent material may be attributable either to mineral aerosol addition (see
664 section 5.2 below), or it may imply that the extremely small residual pool itself records another
665 translocation process and associated Zn isotope fractionation.

666 While we recognize that we cannot rule out a role for other soil sorption sites, our interpretation of
667 the Maui data emphasizes the role of Fe-Mn oxyhydroxides in retaining Cu and Zn in the oxic soils.
668 This emphasis derives from previous work on these samples (e.g. Schuur et al., 2001; Thompson et
669 al., 2007) that documents a sudden loss of the soil Fe oxide pool as well as a prominent shift in Fe
670 isotopes at the point in the rainfall gradient where residual light Cu is seen here to be lost. The
671 scenario described above may also apply to Cu and Zn isotope features of oxic and water-logged
672 soils described previously. In the context of this study we postulate that light isotopes of Cu at 20-
673 30 cm in the Laupahoehoe profile might be explained in terms of mobilization of heavy Cu into
674 aqueous organic complexes in soil solutions and retention of light Fe on residual Fe oxides. Bigalke
675 et al. (2010a) studied a Skeleti-Stagnic Luvisol, with variations in non-crystalline oxides with depth

within the profile related to drained versus water-logged conditions. They also observe a transition from light isotopes of Cu at the surface to heavier isotopes at depth, coupled to an associated drop in Cu concentrations. Bigalke et al. (2010a) attributed this to redox cycling, without settling on a precise explanation. Viers et al. (2007) found similar features to those seen in Maui soils for Zn, in a soil-plant system in a pristine tropical watershed in Cameroon: strong Zn depletion with enrichment in light Zn isotopes (but by up to 0.6‰ in their case) in "ferruginous" horizons, that contrasted with a water-logged "swamp zone" that had Zn isotopes very similar to the bedrock. We also note that this potentially important process controlling Cu, Zn and their isotopes in soils is analogous to that proposed for Fe isotope behaviour in Podzols, where heavy Fe is mobilised into aqueous solutions by organic-ligand-promoted dissolution and complexation, while illuvial B horizons are enriched in the light isotopes by 0.6‰ (Wiederhold et al., 2007).

5.2 The impact of mineral aerosol dust: the example of the Kohala 150 kyr soil profiles

The Hawaiian island soil sites were specifically chosen for their remoteness from sources of anthropogenic and natural contamination via the atmosphere. Though the surfaces of many soils studied here, in both Hawaii and Scotland, often show very significant enrichment in Pb (Tables 1,3), there is no overall relationship between τ_{Pb} and τ_{Cu}, τ_{Zn} or Cu-Zn isotopes, suggesting that anthropogenic impacts on Cu, Zn and their isotopes are not significant in these soils. A recent study of Mo and its isotopes (King et al., 2016) has documented the significance of atmospheric Mo sourced in volcanic fog (vog), but too little is known about the Cu-Zn content of this material to be more precise about its relevance to our study. Many previous studies, however, using tracers such as quartz and mica content (not present in parent basalt but present throughout Hawaiian soils, even at depth within soil profiles, e.g. Kurtz et al., 2001) as well as an array of isotopic and trace element approaches, have documented the importance of Asian dust to the Hawaiian soils (e.g. Kennedy et al., 1998; Teutsch et al., 1999; Kurtz et al., 2001; Stewart et al., 2001; Huh et al., 2004; Monastra et al., 2004; Scribner et al., 2006; Pett–Ridge et al., 2007; Chadwick et al., 2009; Mikutta et al., 2009). Examination of the detailed systematics of the soils studied here reveal the impact of a similar complication for these metals (Fig. 8). The blue and green arrows on the tau-tau plots on Fig. 8 recap the findings for Maui soils described in section 5.1, but also show data for the other Hawaiian soils studied. Clearly, the soils from Laupahohoe and Kohala in particular show deviations from the simple removal trajectories for Cu, Zn and heavy Cu isotopes seen in Maui Site 2 (blue arrows in Fig. 8). The russet arrows on panels (a), (c) and (d) in Fig. 8 illustrate the trajectory that would be observed for a variable supply of Asian dust, using the constraints on its chemistry derived from the

709 study of North Pacific deep sea sediments (Kyte et al., 1993) in a fashion analogous to the approach
710 taken by Pett-Ridge et al. (2007) for uranium.

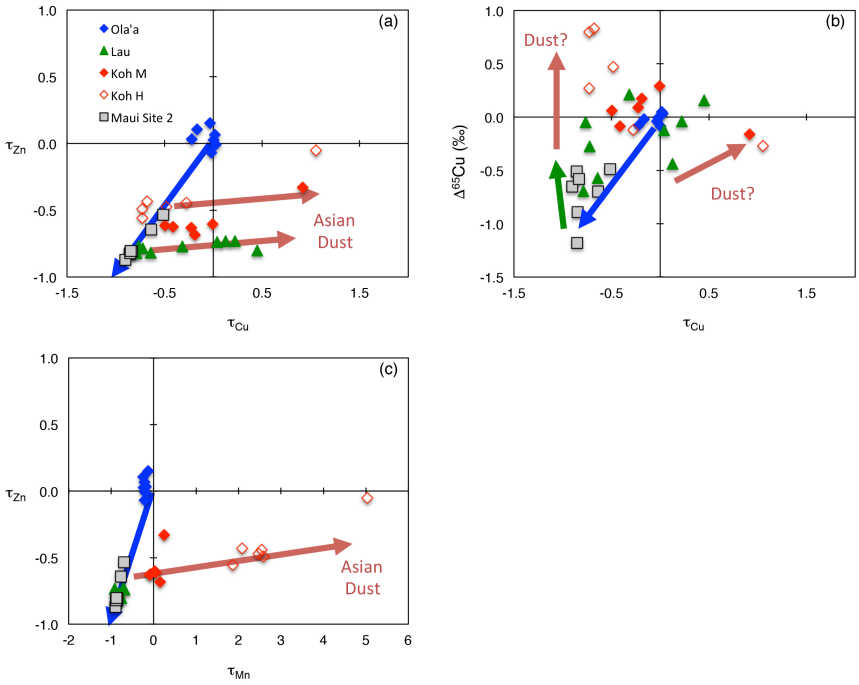

711

712 **Figure 8:** Relationships between τ_{Mn}, τ_{Cu}, τ_{Zn} and Cu isotope compositions Maui Site 2 and all other Hawaiian soils
713 studied here. Site 2 at Maui is shown to illustrate the important process identified there involving coupled loss of Cu
714 and Zn in proportion to their occurrence in parent material, and preferential loss of the light isotope of Cu (blue arrows).
715 Note that Cu isotopic composition in (b) is plotted as a Δ value from parent material. The green arrow on this figure
716 shows schematically the trajectory seen in Sites 4 and 6 at Maui, involving loss of the light Fe-oxide pool of Cu. A
717 trajectory similar to the blue arrow explains a lot of the data from other soils. The prominent exceptions are soils from
718 Kohala, and to a lesser extent Laupahoehoe. The russet arrows on the tau diagrams (a) and (c) and show the trajectory
719 expected through addition of Asian dust (Kyte et al., 1993; Pett-Ridge et al., 2007). The exact trajectory created by such
720 addition on (b) is difficult to estimate, and depends on how much Cu is left in the soil when the dust is added – e.g. if
721 Cu is completely removed from the soil before dust Cu is added the trajectory could be near vertical, whereas the slope
722 will be gentler if the dust is added when there is still significant parent Cu remaining in the soil.

723 The slope of the arrows on Fig. 8 are obtained by calculating a "tau" value for Asian dust relative to
724 the parent material from which the soils derive and then a ratio, e.g. of τ_{Cu} to τ_{Zn} in panel (a). Thus
725 the trajectories illustrate how the chemistry of a soil that had not been chemically weathered at all
726 would respond to dust addition. If two elements plotted on one of these panels are removed by
727 chemical weathering in the proportions they are found in parent material before dust addition, the
728 russet arrows accurately indicate the impact of dust. This is apparently the case for Cu vs. Zn at
729 Maui site 2 (section 5.1), and the blue arrow drawn on Fig. 8c also suggests that it is the case for Zn
730 vs. Mn. As can be seen, the trajectories for dust addition match data arrays well. These dust
731 trajectories are relatively flat on both the τ_{Cu}- τ_{Zn} and τ_{Mn} -τ_{Zn} plots because Hawaiian soils are very
732 depleted in Cu and Mn relative to Asian dust, while Zn concentrations are similar. In other words,
733 the flat trajectory on the Mn-Zn plot results from the very high Mn/Zn ratio of Asian dust relative to

734 Hawaiian soils. Though the Mn addition to the Kohala H soil appears extreme, we note that
735 Kraepiel et al. (2015) document soil τ_{Mn} values up to 6 times higher, which they also attribute to
736 atmospheric addition, possibly in combination with biolifting by plants and the fact that oxidizing
737 conditions lead to retention of dust-derived Mn near the top of the soil. Given the mean annual
738 precipitation of 1060mm at the Kohala H site, and the well-established relationship between MAP
739 and redox, we expect Eh to be well in excess of +500 mV and that Mn should remain in oxidized
740 form.

741 Any attempt to subtract the impact of dust on the Cu and Zn isotopic compositions of the soils it
742 affects is rendered difficult by two issues, as illustrated in the τ_{Cu}-δ^{65}Cu panel (b) of Fig. 8. On this
743 diagram the trajectories that would be defined by samples that have seen dust added are variable
744 because the impact on Cu isotopes depends on the Cu concentration of the soil – how much
745 depletion by chemical weathering it had undergone - when the dust is added. The other problem is
746 that if the isotopic data at Kohala are to be explained by dust addition then that dust must
747 sometimes have a minimum δ^{65}Cu +0.9‰ (Fig. 8b) and a minimum δ^{66}Zn of +0.8‰ (not figured,
748 Table 3). We expect the copper isotope composition of an Asian dust source to approximate that of
749 the continental crust and sediments. This is close to zero in δ^{65}Cu, and measured values for Chinese
750 Loess as well as Atlantic marine aerosols range from -0.2 to +0.3‰ (Li et al, 2009; Little et al.,
751 2014a). δ^{65}Cu values = 0.03±0.12 and 0.20± 0.16‰ and δ^{66}Zn values = 0.20±0.05 and 0.28±0.08
752 ‰ have been reported for the <4μm fractions of dust samples from Taklamakan Desert, China,
753 considered to be a major source of the Asian dust plume (Dong et al., 2013). This study also found
754 variations of up to 0.5‰ among the different size fractions, with some samples of the >63μm
755 fraction notably giving isotopic values 0.37-0.48‰. Copper and zinc in atmospheric dust is likely to
756 be present in metal-rich coatings (desert varnish) on the surfaces of quartz. It is possible that these
757 oxide coatings could have heavy Cu and Zn due to adsorption fractionation, as suggested for iron
758 isotopes on desert varnishes by Busigny and Dauphas (2007). Supergene enriched copper minerals
759 tend to have heavier Cu-isotopic compositions than primary copper minerals (Mathur et al, 2005,
760 2009; Markl et al., 2006; Matthews unpublished data) with values as high as 9.5‰ and their
761 exposure in the surface could bias the dust record.

762 **5.3 Impact of biological cycling on surface horizons of young Glen Feshie soils**

763 The surface horizons of Glen Feshie soils are variably enriched in Cu and Zn. Cu isotopes are
764 generally slightly heavier, while Zn isotopes are subtly lighter than horizons immediately beneath.
765 *A priori* these features could be caused either by deposition of Cu and Zn from the atmosphere onto

766 the surface, of either mineral dust or anthropogenic particulates, or with translocation of Cu and Zn
767 upwards through the soil due to plant activity at the surface. Bigalke et al. (2010a, 2011) discuss
768 both these possibilities with regard to enrichments of Cu in the surface horizons of soils.

769 The field site at Glen Feshie is situated away from major industrial centres. The most likely source
770 of anthropogenic Cu and Zn would therefore be long-range transfer of ash or dust from smelters and
771 refineries. Some deposition at Glen Feshie is possible given the transport distances previously
772 observed for anthropogenic Zn (Candelone et al. 1995; Planchon et al. 2002). The isotopic
773 composition of anthropogenic Cu in ash or dust is highly dependent upon that of the ores being
774 smelted (Mattielli et al. 2009), which can be highly variable (Mathur et al. 2009). Conversely, Zn
775 in ash or dust is light due to evaporation during the smelting process (Mattielli et al. 2009), and is
776 fractionated during atmospheric transport, leading to increasingly light compositions with
777 increasing transport distances (Sonke et al. 2008). Anthropogenic Zn deposited at Glen Feshie
778 would therefore be expected to be isotopically light, as is observed.
779
780 Major deposition of anthropogenic Cu and Zn from smelting has occurred since ~1900 (Thapalia et
781 al. 2010). It follows, therefore, that if significant anthropogenic deposition had occurred at Glen
782 Feshie, all the soils older than ~100 years would be affected to the same extent. This is clearly not
783 the case. τ_{Cu} and τ_{Zn} at Glen Feshie (Fig. 3) show accumulation of both metals at the surface. This
784 could indicate addition of the metals via dust or ash but, since accumulation increases with age and
785 is not the same for all soils older than ~100 years, an anthropogenic origin does not seem likely.
786 Furthermore, the trend towards lighter isotopic compositions of Zn at Glen Feshie is progressive
787 with age rather than a step change between the 0.1ka and older soils (Fig. 3).
788
789 Additional Cu and Zn could also be derived from mineral aerosols. But Nd data for Glen Feshie
790 (Keech 2011) suggest no significant accumulation of mineral aerosols. This is supported by simple
791 estimates of dust input to Glen Feshie. Modelling by Mahowald (2006) suggests a present-day rate
792 of dust deposition over Scotland of 0.75±0.25 $g/m^2/yr$. Using this rate and assuming concentrations
793 of Cu and Zn in dust equal to their concentrations in the upper continental crust (25 and 71 ppm
794 respectively; Taylor and McClennan, 1995), then the total masses of Cu and Zn deposited on the
795 Glen Feshie soils over 13 ka are 0.24 and 0.69 g/m^2 respectively. These values are equivalent to
796 about 5% and 2% of the total amount of Cu and Zn in the uppermost metre of the 13 ka soil
797 (assuming a density of 1000 g/m^3). These estimates confirm that mineral aerosols must constitute,
798 at most, a minor input of Cu and Zn to these soils and, combined with an apparent lack of

anthropogenic input, we propose that vegetation and weathering are the dominant controls upon cycling of Cu and Zn in organic-rich shallow soils horizons at Glen Feshie.

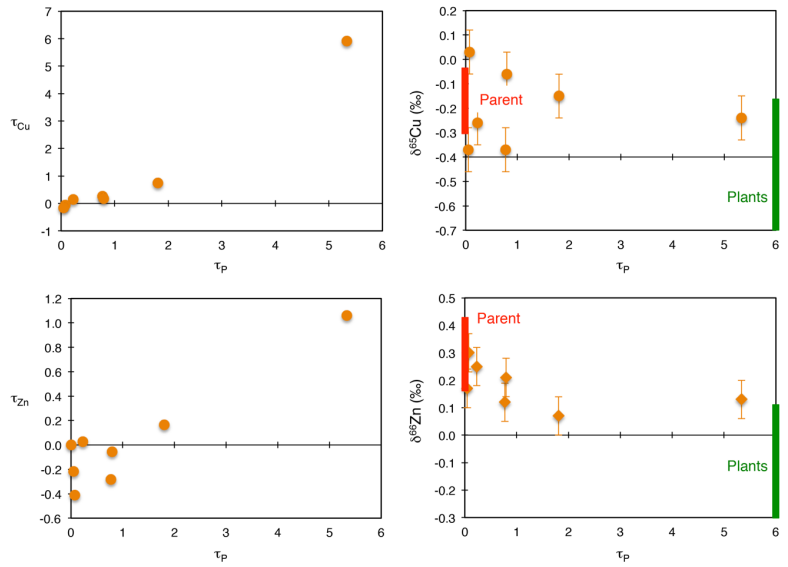

Figure 9: Relationships between τ_P τ_{Cu}, τ_{Zn} and Cu-Zn isotope compositions for the upper organic-rich levels of Glen Feshie soils., showing coupled enrichment of phosphorous and Cu (top left) and Zn (bottom left). Such biological concentration of Cu and Zn in surface horizons may come with lighter Zn isotopes (bottom right), but data for Cu isotopes does not indicate any particular trend.

Schulz et al. (2010) observed the effect of biolifting on the distribution and composition of Fe in a soil chronosequence from Santa Cruz, California. Biolifting is the process by which plant roots and symbiotic fungi (mycorrhizae) transport an element from deep in the regolith to the shallow soil. The τ_{Cu} and τ_{Zn} and τ_P (Fig. 3) profiles observed at Glen Feshie are indicative of biolifting. τ_{Zn} increases with soil age in the uppermost soil horizons but decreases at depth, suggesting movement of Zn upwards with increasing soil development. Moreover, τ_{Cu} and τ_{Zn} are correlated with τ_P, as demonstrated in Fig. 9. *Calluna vulgaris* is strongly mycorrhizal, and therefore biolifting provides a likely explanation for the distribution of Zn observed at Glen Feshie. Enrichment of Cu is also seen at the surface of the Glen Feshie soils. Biolifting and fractionation by vegetation can also explain some aspects of soil $\delta^{66}Zn$ and $\delta^{65}Cu$ at Glen Feshie. Plant samples from Glen Feshie demonstrate a preference for light Cu and Zn (Table 2). This is broadly in keeping with the observations of previous studies, but also with some important differences as discussed earlier in section 4.1 The general trend towards lighter Zn with τ_P (Fig. 9) may reflect the preferential movement of light Zn upwards through the soil profile facilitated by mycorrhizae. Additional light Zn at the surface could come from leaf litter and the decay of dead plant matter enriched in the light isotopes. Conversely however, one might expect plant uptake of the light isotopes to leave soils enriched in heavy Zn.

This type of process could explain the trend towards heavier $\delta^{65}Cu$ values at the surface of the soil profiles (Fig. 3). The relative impact of these processes is unknown, as total biomass per unit soil has not been measured for the Glen Feshie soils, but their dual control could explain the absence of a relationship between τ_P and Cu isotopes seen in Fig. 9. Overall, a more definitive identification of the process of bio-lifting for Cu and Zn and their isotopes must await more targeted studies than possible here.

6. Concluding remarks: Integrated soil Cu-Zn isotopes and the isotopic composition of rivers

In this concluding section we return to our larger-scale objective in this paper, to investigate the extent to which processes in soils can explain observations of heavy Cu isotopes relative to rocks, in contrast with relatively unfractionated Zn isotopes, in the dissolved phase of rivers. To do so we calculate values of tau for elements of interest, integrated for entire soil profiles, weighting taus for individual horizons for density (ρ) (where data are available) and thickness (z) as follows:

$$\tau_i^{int} = \sum \frac{\left(\tau_h \rho_h z_h\right)}{\left(\rho_t z_t\right)}$$

where *h* refers to each individual horizon and *t* to the values for the entire profile. Unfortunately, density data are not available for the Glen Feshie or Kohala H samples, and we are forced to calculated integrated taus without weighting for the density of each horizon. Figure 10 plots these data versus integrated soil $\Delta^{65}Cu_{\text{parent material-soil}}$ and $\delta^{66}Zn_{\text{parent material-soil}}$. On these diagrams the lower left quadrant denotes loss of heavy isotopes from soils while the upper left quadrant denotes loss of light isotopes.

We have discussed an array of fundamental soil geochemistry processes that determine the fate of Cu and Zn in coarse- and fine-grained granitic and basaltic soils, respectively. Isotopically light Cu is retained on Fe oxyhydroxides in the least reduced Maui soil profile, while reduction of Fe oxides at the wetter sites strips out this residual light Cu under anaerobic conditions. Though there has presumably been addition of mineral aerosol to the Maui soils, Cu-Zn isotopes appear to be dominated by depletion processes. At Kohala in particular, on the other hand, these chemical weathering processes are overprinted by the addition of mineral aerosol dust. In the young Scottish soils, bio-lifting of Cu and Zn to surface horizons is an important process. Nevertheless, and despite these complexities, it is clear from Fig. 10 that, overall, isotopically heavy Cu is lost from soils, while integrated isotopic compositions of Zn in soils do not depart significantly from those of

parent material. The trajectories for addition of Asian dust illustrated in Fig. 8 could, in principle, allow us to remove this overprint from the older Hawaiian soils. Unfortunately, however, quantitative correction is precluded by the lack of constraint on the Cu isotopic composition of the added mineral aerosol. What can be concluded for sure, however, is that the Cu added by mineral aerosol is isotopically heavy, so that the degree to which weathering and other processes cause enrichment of light Cu in soils, and the export of heavy isotopes, is under-emphasised in Fig. 10.

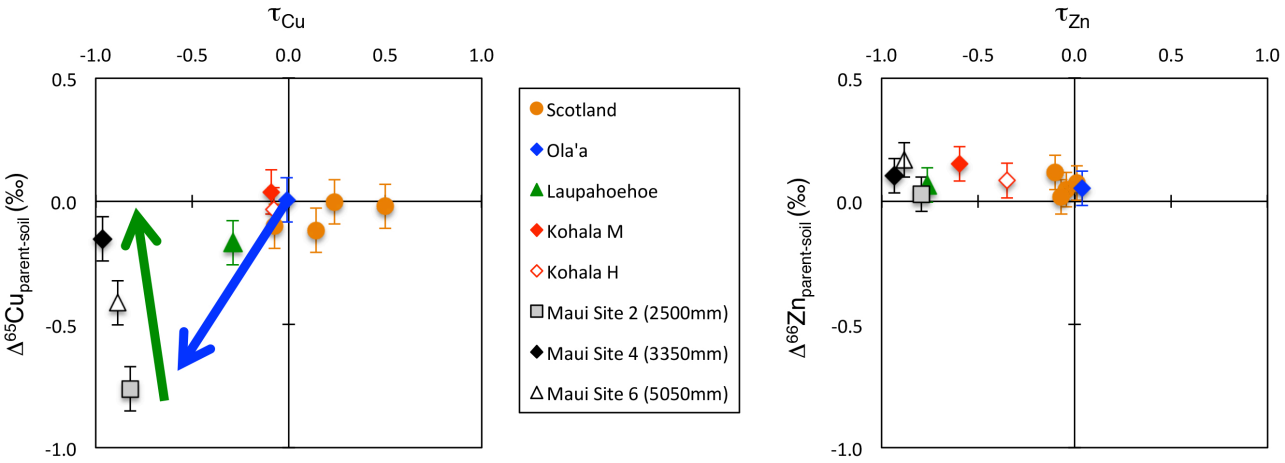

Figure 10: Integrated (whole-profile) taus and isotopic compositions for the soils studied here, with Zn isotopes plotted on the same scale as Cu to illustrate the relative subtlety of Zn isotope variation in soils. The blue and green arrows indicate the weathering processes identified in the Maui rainfall sequence identified earlier: retention of light residual Cu isotopes on Fe oxides in oxic soils (blue), loss of this pool in water-logged soils (green). Weathering loss of light isotopes of Cu, however, is obscured in other locations due to addition of heavy dust-derived Cu (Kohala, Hawaii), while the Scottish soils also appear to have accumulated Cu. All soils have lost Zn but with insignificant isotope fractionation.

We suggest, however, that the weathering process identified in the oxic soils of Maui, involving the partitioning of stable isotopes between aqueous organic complexes and particulate oxyhydroxide surfaces, is likely to be a key factor in the behaviour of metal isotopes in soils and elsewhere at the surface of the Earth. In low ionic strength aqueous solutions, experiments suggest subdued isotopic fractionation via sorption from an inorganic Zn pool (Bryan et al., 2015), which may be negated or reversed if the aqueous Zn pool is complexed by organic ligands (Jouvin et al., 2009), as seen here for soils and for rivers in Little et al. (2014a). The more pronounced preference of these organic complexes for heavy isotopes (Ryan et al., 2014) probably causes the larger fractionations seen for Cu in oxic soils (this study), and in the dissolved versus particulate pool of rivers (Vance et al., 2008). The higher ionic strength of the oceans, on the other hand, coupled to organic speciation of both Cu and Zn in the aqueous phase, produces smaller fractionations for Cu (e.g. Vance et al., 2008; Little et al. 2014a,b) and significantly heavy Zn isotopes sorbed on oxyhydroxides relative to

the dissolved pool (e.g. Marechal et al., 2000; Vance et al., 2008; Zhao et al., 2014; Conway and John, 2014; Little et al., 2014a,b; Bryan et al., 2015).

So it is clear that the isotopic characteristics of the dissolved pool of rivers (Vance et al., 2008; Little et al., 2014a) can be rationalised by processes that at least start in soils. Nevertheless, there is a mass balance issue to be considered. Neubert et al. (2011) pointed out that soils cannot be the ultimate long-term storage reservoir for the isotopically light particulate-bound Mo that is required to balance the isotopically heavy riverine Mo flux. The same is true for Cu and Zn, as illustrated by a simple order of magnitude calculation. If we use the Maui Cu and Zn concentrations and soil densities, and if we calculate the Cu and Zn inventories in 1m of soil spread over the entire extra-Antarctic continental area, we find that soils could store only about 30 years worth of the riverine flux of Cu, and about 125 years worth of the riverine flux of Zn. These figures are almost certainly maxima: soils cannot be the ultimate storage reservoirs of the light Cu required to balance rivers. At Glen Feshie, and in the small river studied in detail by Vance et al. (2008), riverine particulates are also isotopically light. The ultimate storage reservoir is likely, then, to be fluvial and continental margin sediments. The fate of the oxyhydroxide-associated Cu that might be stored in these settings, against diagenetic processes that potentially re-mobilise it into the oceanic dissolved pool (e.g. Shaw et al. 1990), will be important for oceanic mass and isotopic balances (e.g. Little et al., 2014a,b), and a target for future work.

Acknowledgements

Some of the research in this contribution was funded by NERC grant NE/G009961/1 to DV. AM received support from Israel Science Foundation grant 1140/12. We thank three anonymous reviewers for comments that significantly improved the manuscript, and we acknowledge the efforts of the guest editors in putting together this special issue.

References

Archer, C., Vance, D., 2004. Mass discrimination in plasma source mass spectrometry: an example using Cu and Zn isotopes. J. Anal. Atom. Spectrom. 19, 656-665.

Archer, C., Vance, D., 2008. The isotopic signature of the global riverine molybdenum flux and anoxia in the ancient oceans. Nature Geoscience 1, 597-600.

Arnold, T., Kirk, G.J.D., Wissuwa, M., Frei, M., Zhao, F.J., Mason, T.F.D., Weiss, D.J., 2010. Evidence for the mechanisms of zinc uptake by rice using isotopic fractionation. Plant Cell Environ. 33, 370-381.

Bain, D.C., Mellor, A., Robertson-Rintoul, M.S.E., Buckland, S. T., 1993. Variations in weathering processes and rates with time in a chronosequence of soils from Glen Feshie Scotland. Geoderma 57, 275-293.

Balistrieri, L.S., Borrok, D.M., Wanty, R.B, Ridley, W.I., 2005. Fractionation of Cu and Zn isotopes during adsorption onto amorphous Fe(III) oxyhydroxide: experimental mixing of acid rock drainage and ambient river water. Geochim. Cosmochim. Acta 72, 311-328.

Barling, J., Arnold, G.L., Anbar, A.D., 2001. Natural mass-dependent variations in the isotopic composition of molybdenum. Earth Planet. Sci. Lett. 193, 447-457.

Barling, J., Anbar, A.D., 2004. Molybdenum isotope fractionation during adsorption by manganese oxides. Earth Planet. Sci. Lett. 217, 315-329.

Bermin, J., Vance, D. Archer, C., Statham, P.J., 2006. The determination of the isotopic composition of Cu and Zn in seawater. Chem. Geol. 226, 280-297.

Bigalke, M., Weyer, S., Wilcke, W., 2010a. Stable copper isotopes: a novel tool to trace copper behaviour in hydromorphic soils. Soil Sci. Soc. Amer. J. 74, 60-73.

Bigalke, M., Weyer, S., Wilcke, W., 2010b. Copper isotope fractionation during complexation with insolubilized humic acid. Environ. Sci. Tech. 44, 5496-5502.

Bigalke, M., Weyer, S., Wilcke, W., 2011. Stable Cu isotope fractionation in soils during oxic weathering and podzolisation. Geochim. Cosmochim. Acta 75, 3119-3134.

Bryan, A.L., Dong, S., Wilkes, E.B., Wasylenki, L.E., 2015. Zinc isotope fractionation during adsorption onto Mn oxyhydroxide at low and high ionic strength. Geochim. Cosmochim. Acta 157, 182-197.

Busigny, V, Dauphas, N., 2007. Tracing paleofluid circulations using iron isotopes: a study of hematite and goethite concretions from the Navajo Sandstone (Utah, USA). Earth Planet. Sci. Lett. 254, 272-287.

Cameron, V., Vance, D., 2014. Heavy nickel isotope compositions in rivers and the oceans. Earth Planet. Sci. Lett. 128, 195-211.

Candelone, J. P., Hong, S. M., Pellone, C., Boutron, C. F., 1995. Post-Industrial Revolution changes in large scale atmospheric-pollution of the North Hemisphere by heavy metals as documented in central Greenland snow and ice. J. Geophys. Res. Atmospheres 100, 16605-16616.

Chadwick O.A., Brimhall G.H., Hendricks D.M., 1990. From a black box to a gray box - a mass balance interpretation of pedogenesis. Geomorphology 3, 369–390.

Chadwick O.A., Derry L.A., Vitousek P.M., Huebert B.J., Hedin L.O., 1999. Changing sources of nutrients during four million years of ecosystem development. Nature 397, 491-497.

Chadwick, O.A., Chorover, J., 2001. The chemistry of pedogenic thresholds. Geoderma 100, 321–

353.

Chadwick O.A., Gavend R.T., Kelly E.F., Ziegler K., Olson C.G., Elliott W., Hendricks. D.M., 2003. The impact of climate on the biogeochemical functioning of volcanic soils. Chem. Geol. 202, 195– 223.

Chadwick, O.A., Derry, L.A., Bern, C.R., Vitousek, P.M., 2009. Changing sources of strontium to soils and ecosystems across the Hawaiian Islands. Chem. Geol. 267, 64-76.

Chen, H., Savage, P.S., Teng, F.-Z., Helz, R.T., Moynier, F., 2013. Zinc isotope fractionation during magmatic differentiation and the isotopic composition of the bulk Earth. Earth Planet. Sci. Lett. 369-370, 34-42.

Chen, J., Gaillardet, J., Louvat, P., 2008. Zinc isotopes in the Seine River waters France: a probe of anthropogenic contamination. Environ. Sci. Technol. 42, 6494-6501.

Chen, J.-B., Gaillardet, J., Bouchez, J., Louvat, P., Wang, Y.-N., 2014. Anthropophile elements in river sediments: overview from the Seine River, France. Geochem. Geophys. Geosyst. 15, 4526-4546.

Chorover, J., DiChiaro, M.J., Chadwick, O.A., 1999. Structural charge and cesium retention in a chronosequence of tephritic soils. Soil Sci. Soc. Am. J. 63, 169–177.

Conway, T.M., John, S.G., 2014. The biogeochemical cycling of zinc and zinc isotopes in the North Atlantic Ocean. Glob. Biogeochem. Cyc. 28, 1111-1128.

Crews, T.E., Kitayama, K., Fownes, J.H., Riley, J.H., Herbert, D.A., Mueller-Dombois, D., Vitousek, P.M., 1995. Changes in soil phosphorus fractions and ecosystem dynamics across a long chronosequence in Hawaii. Ecology 76, 1407-1424.

Dong, S., Weiss, D. J., Strekopytov, S., Kressig, K., Sun, Y., Baker, A.R., Formenti, P., 2013. Stable isotope measurement of Cu and Zn in mineral dust (bulk and size fractions) of the Taklimakan Desert and the Sahel and in aerosols from the eastern tropical North Atlantic Ocean. Talanta 114, 103-109.

Fujii, T., Moynier, F., Blichert-Toft, J., Albarede, F., 2014. Density functional theory estimation of isotope fractionation of Fe, Ni, Cu and Zn among species relevant to geochemical and biological environments. Geochim. Cosmochim. Acta 140, 553-576.

Grybos, M., Davranche, M., Gruau, G., Petitjean, P., 2007. Is trace metal release in wetland soils controlled by organic matter mobility or Fe-oxyhydroxides reduction? J. Colloid Interface Sci. 314, 490-501.

Helliwell, R.C., Ferrier R.C., Kernan, M.R., 2001. Interaction of nitrogen deposition and land use on soil and water quality in Scotland: issues of spatial variability and scale. Sci.Total Environ. 265, 51-63.

Hodson, M.E., Langan, S.J., Kennedy, F.M., Bain, D.C., 1998. Variation in soil surface area in a chronosequence of soils from Glen Feshie Scotland and its implications for mineral weathering rate calculations. Geoderma 85, 1-18.

Hodson, M.E., Langan, S.J., 1999. The influence of soil age on calculated mineral weathering rates. App. Geochem. 14, 387-394.

Hotchkiss, S., Vitousek, P.M., Chadwick, O.A., Price, J., 2000. Climate cycles, geomorphological history and the interpretation of soil and ecosystem development. Ecosystems 3, 522–533.

Huh, Y., Chan, L-H., Chadwick, O.A., 2004. Behavior of lithium and its isotopes during weathering of Hawaiian basalt. Geochem. Geophys. Geosystems 5, doi:10.1029/2004GC000729.

990 Keech, A.R., 2011. Chemical weathering in an icehouse world: the record from soils and lakes.
991 Ph.D. Thesis, University of Bristol, 202 pp.

992 King, E.K., Thompson, A., Chadwick, O.A., Pett-Ridge, J.C., 2016, Molybdenum sources and
993 isotopic composition during early stages of pedogenesis along a basaltic climate transect. Chem.
994 Geol., in press.

995 Kraepiel, A.M.L., Dere, A.L., Herndon, E.M., Brantley, S.L., 2015. Natural and anthropogenic
996 processes contributing to metal enrichment in surface soils of central Pennsylvania. Biogeochem.
997 123, 265-283.

998 Kusonwiriyawong, C., Bigalke, M., Abgottspon, F., Lazarov, M., Wilcke, W., 2016. Response of
999 Cu partitioning to flooding: a δ^{65}Cu approach in a carbonatic alluvial soil. Chem. Geol. 420, 69-76.

1000 John, S.G., Park, J.G., Zhang, Z., Boyle, E.A., 2007. The isotopic composition of some common
1001 forms of anthropogenic zinc. Chem. Geol. 245, 61-69.

1002 Juillot, F., Maréchal, C., Ponthieu, M., Cacaly, S., Morin, G., Benedetti, M., Hazemann, J.L., Proux,
1003 O., Guyot, F., 2008. Zn isotopic fractionation casued by sorption on goethite and 2-Lines
1004 ferrihydrite. Geochim. Cosmochim. Acta 72, 4886-4900.

1005 Juillot, F., Maréchal, C., Morin, G., Jouvin, D., Cacaly, S., Telouk, P., Benedetti, M.F., Ildefonse,
1006 P., Sutton, S., Guyot, F., Brown, G.E., 2011. Contrasting isotopic signatures between anthropogenic
1007 and geogenic Zn and evidence for post-depositional fractionation processes in smelter-impacted
1008 soils from Northern France. Geochim. Cosmochim. Acta 75, 2295-2308.

1009 Jouvin, D., Louvat, P., Juillot, F., Maréchal, C.N., Benedetti, M.F., 2009. Zinc isotopic
1010 fractionation: why organic matters. Environ. Sci. Technol. 43, 5747-5754.

1011 Keller, C, Domergue, F.L. 1996. Soluble and particulate transfers of Cu, Cd, Al, Fe and some major
1012 elements in gravitational waters of a Podzol. Geoderma 71, 263-274.

1013 Kennedy, M.J., Chadwick, O.A., Vitousek, P.M., Derry, L.A., Hendricks, D.M., 1998 Changing
1014 sources of base cations during ecosystem development, Hawaiian Islands. Geology 26, 1015–1018.

1015 Kurtz, A.C., Derry, L.A., Chadwick, O.A., Alfano, M.J., 2000. Refractory element mobility in
1016 volcanic soils. Geology 28, 683–686.

1017 Kurtz, A.C., Derry, L.A., Chadwick, O.A., 2001. Accretion of Asian dust to Hawaiian soils:
1018 Isotopic, elemental, and mineral mass balances. Geochim. Cosmochim. Acta 65, 1971–1983.

1019 Kyte, F.T., Leinen, M., Heath, G.R., Zhou, L., 1993. Cenozoic sedimentation history of the central
1020 North Pacific: inferences from the elemental geochemistry of core LL44-GPC3. Geochim.
1021 Cosmochim. Acta 57, 1719-1740.

1022 Lee, M.R., Brown, D.J., Hodson, M.E., MacKenzie, M., Smith, C.L., 2008. Weathering
1023 microenvironments on feldspar surfaces: implications for understanding fluid-mineral reactions in
1024 soils. Mineral. Mag. 72, 1319-1328.

1025 Li, W., Jackson, S.E., Pearson, N.J., Alard, O., Chappell, B.W., 2009. The Cu isotopic signature of
1026 granites from the Lachlan Fold Belt, SE Australia. Chem. Geol. 258 38–49

1027 Little, S.H. Vance, D., Walker-Brown, C., Landing, W.M., 2014a. The oceanic mass balance of
1028 copper and zinc isotopes, investigated by analysis of their inputs and oxic output in ferromanganese
1029 crusts. Geochim. Cosmochim.Acta 125, 673-693.

1030 Little, S.H., Sherman, D.M., Vance, D., Hein, J.R., 2014b. Molecular controls on Cu and Zn
1031 isotopic fractionation in Fe-Mn crusts. Earth Planet. Sci. Lett. 396, 213-222.

1032 Liu, S.-A., Huang, J., Liu, J., Wörner, G., Yang, W., Tang, Y.-J., Chen, Y., Tang, L., Zheng, J., Li,

S., 2015. Copper isotopic composition of the silicate Earth. Earth Planet. Sci. Lett. 427, 95-103.

Mahowald, N. M., Muhs, D. R., Levis, S., Rasch, P. J., Yoshioka, M., Zender, C. S., Luo, C., 2006. Change in atmospheric mineral aerosols in response to climate: Last glacial period preindustrial modern and doubled carbon dioxide climates. J. Geophys. Res. 111, D10202, doi:10. 1029/2005JD006653.

Maréchal, C.N., Nicolas, E., Douchet, C., Alvarede, F., 2000. Abundance of zinc isotopes as a marine biogeochemical tracer. Geochem. Geophys. Geosys. 1, 10.1029/1999GC000029.

Markl, G., Lahaye, Y., Schwinn, G., 2006. Copper isotopes as monitors of redox processes in hydrothermal mineralization. Geochim. Cosmochim. Acta 70, 4215–4228.

Mathur, R., Ruiz, J., Titley, S., Liermann, L., Buss, H., Brandtley, S., 2005. Cu isotopic fractionation in the supergene environment with and without bacteria. Geochim. Cosmochim. Acta 69, 5233–5246.

Mathur, R., Titley, S., Barra, F., Brantley, S., Wilson, M., Phillips, A., Munizaga, F., Maksaev, V., Vervoort J., Hart G., 2009. Exploration potential of Cu isotope fractionation in porphyry copper deposits. J. Geochem. Explor. 102, 1-6.

Mattielli, N., Rimetz, J., Petit, J., Perdrix, E., Deboudt, K., Flament, P., Weis, D., 2009. Zn-Cu isotopic study and speciation of airborne metal particles within a 5-km zone of a lead/zinc smelter. Geochim. Cosmochim. Acta 70, A401-A401.

McPhie, J., Walker, G.P.L., Christiansen R.L., 1990. Phreatomagmatic and phreatic fall and surge deposits from explosions at Kilauea Volcano, Hawaii, 1790 AD — Keanakakoi Ash Member. Bull. Volcanol. 52, 334–354.

Monastra, V., Derry, L.A., Chadwick O.A., 2004. Multiple sources of lead in soils from a Hawaiian chronosequence. Chem. Geol. 209, 215–231.

Mikutta, R., Schaumann, G.E., Gildemeister, D., Bonneville, S., Kramer, M.G., Chorover, J., Chadwick, O.A., Guggenberger G., 2009. Biogeochemistry of mineral–organic associations across a long term mineralogical soil gradient (0.3–4100 kyr), Hawaiian Islands. Geochim. Cosmochim. Acta 73 2034–2060.

Miller, A.J., Schuur, E.A.G., Chadwick, O.A., 2001. Redox control of phosphorous pools in Hawaiian montane forest soils. Geoderma 102, 219-237.

Moynier, F., Pichat, S., Pons, M.-L., Fike, D., Balter, V., Albarede, F., 2009. Isotopic fractionation and transport mechanisms of Zn in plants. Chem. Geol. 267, 125-130.

Moynier, F., Vance, D., Fujii, T., Savage, P., 2016. This isotope geochemistry of zinc and copper. Rev. Mineral. Geochem., in press.

Nakagawa, Y., Takano, S., Firdhaus, M.L., Norisuye, K., Hirata, T., Vance, D., Sohrin, Y., 2012. The molybdenum isotopic composition of the modern ocean. Geochem. J. 46, 131-141.

Neubert, N., Heri, A.R., Voegelin, A.R., Nägler, T.F. Schlunegger, F., Villa, I.M. 2011. The molybdenum isotopic composition in river water: constrains from small catchments. Earth Planet. Sci. Lett. 304, 180-190.

Pett-Ridge, J.C., Monastram V.M., Derry, L.A., Chadwick, O.A., 2007. Importance of atmospheric inputs and Fe-oxides in controlling soil uranium budgets and behavior along a Hawaiian chronosequence. Chem. Geol. 244, 691–707.

1074 Planchon, F. A. M., Boutron, C. F., Barbante, C., Cozzi, G., Gaspari, V., Wolff, E. W., Ferrari, C.
1075 P., Cescon, P. 2002. Changes in heavy metals in Antarctic snow from Coats Land since the mid-
1076 19th to the late-20th century. Earth Planet. Sci. Lett. 200, 207-222.

1077 Pokrovsky, O.S., Biers, J., Freydier, R., 2005. Zinc stable isotope fractionation during its adsorption
1078 on oxides and hydroxides. J. Colloid Interface Sci. 291, 192-200.

1079 Robertson-Rintoul, M.S.E., 1986a. A quantitative soil-stratigraphic approach to the correlation and
1080 dating of post-glacial river terraces in Glen Feshie Western Cairngorms. Earth Surf. Proc.
1081 Landforms 11, 605-617.

1082 Robertson-Rintoul, M.S.E., 1986b. River planform soil stratigraphy and the temporal and
1083 palaeoenvironmental significance of terraced valley fill deposits in upland Scotland with specific
1084 reference to Glen Feshie south-west Cairngorms. Ph.D. thesis, Univ. Hull.

1085 Ryan, B.N., Kirby, J.K., Degryse, F., Scheiderich, K., McLaughlin, M.J., 2014. Copper isotope
1086 fractionation during equilibration with natural and synthetic ligands. Environ. Sci. Technol. 48,
1087 8620-8626.

1088 Schulz, M. S., Bullen, T. D., White, A. F., Fitzpatrick, J. F., 2010. Evidence of iron isotope
1089 fractionation due to biologic lifting in a soil chronosequence. Geochim. Cosmochim. Acta 74,
1090 A927.

1091 Schuur, E.A.G., Chadwick, O.A., Matson, P.A., 2001. Carbon cycling and soil carbon storage in
1092 mesic to wet Hawaiian montane forests. Ecology 82, 3182– 3196.

1093 Scribner, A.M., Kurtz, A.C., Chadwick, O.A., 2006. Germanium sequestration by soil: targeting the
1094 roles of secondary clays and Fe-oxyhydroxides. Earth Planet. Sci. Lett. 243, 760-770.

1095 Shaw, T.J., Gieskers, J.M., Jahnke, R.A., 1990. Early diagenesis in differing depositional
1096 environments: the response of transition meals in pore water. Geochim. Cosmochim. Acta 54, 1233-
1097 1246.

1098 Siebert, S., Pett-Ridge, J.C., Opfergelt, S., Guicharnaud, R.A., Halliday, A.N., Burton, K.W., 2015.
1099 Molybdenum isotope fractionation in soils: influence of redox conditions, organic matter, and
1100 atmospheric inputs. Geochim. Cosmochim. Acta 162, 1-24.

1101 Sivry, Y., Riotte, J., Audry, S., Schäfer, J., Viers, J., Blanc, G., Freydier, R., Dupré, B., 2008. Zn
1102 isotopes as tracers of anthropogenic pollution from Zn-ore smelters: the Riou Mort-Lot river
1103 system. Chem. Geol. 255, 295-304.

1104 Sonke, J. E., Sivry, Y., Viers, J., Freydier, R., Dejonghe, L., Andre, L., Aggarwal, J. K., Fontan, F.,
1105 Dupre B., 2008. Historical variations in the isotopic composition of atmospheric zinc deposition
1106 from a zinc smelter. Chem. Geol. 252, 145-157.

1107 Stewart, B.W., Capo, R.C., Chadwick, O.A., 2001. Effects of rainfall on weathering rate, base
1108 cation provenance, and Sr isotope composition of Hawaiian soils. Geochim. Cosmochim. Acta 65,
1109 1087–1099.

1110 Takano, S., Tanimazu, M., Hirata, T., Sohrin, Y., 2014. Isotopic constraints on biogeochemical
1111 cycling of copper in the ocean. Nature Comms. 10.1038/ncomms6663.

1112 Taylor, S. R., McLennan, S. M., 1995. The Geochemical evolution of the continental crust. Rev.
1113 Geophys. 33, 241-265.

1114 Teutsch, N., Erel, Y., Halicz, L., Chadwick, O.A., 1999. The influence of rainfall on metal
1115 concentration and behavior in the soil. Geochim. Cosmochim. Acta 63, 3499-3511.

1116 Thapalia, A., Borrok, D.M., van Metre, P.C., Musgrove, M., Landa, E.R., 2010. Zn and Cu isotopes
1117 as tracers of anthropogenic contamination in a sediment core from an urban lake. Environ. Sci.
1118 Technol. 44, 1544-1550.

1119 Thompson, A., Rancourt, D.G., Chadwick, O.A., and Chorover, J., 2011. Iron solid phase
1120 differentiation along a redox gradient in basaltic soils. Geochim. Cosmochim. Acta 75, 119-133.

1121 Thompson, A., Ruiz, J., Chadwick, O.A., Titus, M. Chorover J., 2007. Rayleigh fractionation of
1122 iron isotopes during pedogenesis along a climate sequence of Hawaiian basalt. Chem. Geol. 238,
1123 72–83.
1124 Torn, M. S., Trumbore, S. E., Chadwick, O.A., Vitousek, P.M., Hendricks, D.M., 1997. Mineral
1125 control of soil organic carbon storage and turnover. Nature 389, 170–173.

1126 Van Breemen, N., Buurman, P., 2004. Soil Formation. Kluwer Academic Press, Dordrecht,
1127 Netherlands.

1128 Vance, D., Archer, C., Bermin, J., Perkins, J., Statham, P.J., Lohan, M.C., Ellwood, M.J., Mills,
1129 R.A., 2008. The copper isotope geochemistry of rivers and the oceans, Earth Planet. Sci. Lett. 274,
1130 204-213.

1131 Viers, J., Oliva, P., Nonell, A., Gelabert, A., Sonke, J.E., Freydier, R., Gainville, R., Dupre, B.,
1132 2007. Evidence for Zn isotopic fractionation in a soil-plant system of a pristine tropical watershed
1133 (Nsimi Cameroon). Chem. Geol. 239, 124-137.

1134 Vitousek, P.M., 2004. Nutrient Cycling and Limitation: Hawaii as a Model System. Princeton
1135 University Press, 223pp.

1136 Voegelin, A.R., Nägler, T.F., Pettke, T., Neubert, N., Steinmann, M., Pourret, O., Villa, I.M., 2012.
1137 The impact of bedrock weathering on the Mo isotopic composition of stream waters: natural
1138 samples and laboratory experiments. Geochim. Cosmochim. Acta 86, 150-165.

1139 Wasylenki, L.E., Weeks, C.L., Bargar, J.R, Spiro, T.G., Hein, J.R., Anbar, A.D., 2011. The
1140 molecular mechanism of Mo isotope fractionation during adsorption to birnessite. Geochim.
1141 Cosmochim. Acta 75, 5019-5031.

1142 Weber, F.-A., Voegelin, A., Kretzschmar, R., 2009. Multi-metal contaminant dynamics in
1143 temporally flooded soil under sulphate limitation. Geochim. Cosmochim. Acta 73, 5513-5527.

1144 Weber, F.-A., Hofacker, A.F., Voegelin, A., Kretzschmar, R., 2010. Temperature dependence and
1145 coupling of iron and arsenic reduction and release during flooding of a contaminated soil. Environ.
1146 Sci. Technol. 44, 116-122.

1147 Weinstein,C. Moynier, F., Wang, K., Paniello, R., Foriel, J., Catalano, J., Pichat, S., 2011. Isotope
1148 fractionation of Cu in plants. Chem. Geol. 286, 266-271.

Weiss, D.J., Mason,T.F.D., Zhao, F.J., Kirk, G.J.D., Coles, N.J., Horstwood, M.S.A., 2005. Isotopic discrimination of zinc in higher plants. New Phytol. 165, 703-710.

Weiss, D.J., Rausch, N., Mason, T.F.D., Coles, B.J., Wilkinson, J.J., Ukonmaanaho, L., Arnold, T., Nieminen, T.M., 2007. Atmospheric deposition and isotope biogeochemistry of zinc in ombrotrophic peat. Geochim. Cosmochim. Acta 71, 3498-3517.

Wiederhold, J.G., Teutsch, N., Kraemer, S.M., Halliday, A.N., Kretzschmar, R., 2007. Iron isotope fractionation in oxic soils by mineral weathering and podzolisation. Geochim. Cosmochim. Acta 71, 5821-5833.

YeghWebericheyan, D., et al., 2013. A compilation of silicon, rare earth element and twenty-one other trace element concentrations in the natural river water reference material SLRS-5 (NRC-CNRC). Geostand. Geoanal. Res. 37, 449-467.

Zhao, Y., D. Vance, D., Abouchami, W., de Baar, H.J.W., 2014. Biogeochemical cycling of zinc and its isotopes in the Southern Ocean, Geochim. Cosmochim. Acta 125, 653-672.

Ziegler, K., Chadwick, O.A., Berzezinski, M.A., Kelly, E.F., 2005. Natural variations of $\delta^{30}Si$ during progressive basalt weathering, Hawaiian Islands. Geochim. Cosmochim. Acta 69, 4597-4610.